Visual Neuroscience (2007), **24**, 691–707. Printed in the USA.

DOI: 10.1017/S0952523807070599

Projections of the nucleus of the basal optic root in pigeons (*Columba livia*): A comparison of the morphology and distribution of neurons with different efferent projections

DOUGLAS R.W. WYLIE,[1,2] JANELLE M.P. PAKAN,[2] CAMERON A. ELLIOTT,[2] DAVID J. GRAHAM,[2] AND ANDREW N. IWANIUK[1]

[1]Department of Psychology, University of Alberta, Edmonton, Alberta, Canada
[2]University Centre for Neuroscience, University of Alberta, Edmonton, Alberta, Canada

(RECEIVED April 18, 2007; ACCEPTED July 10, 2007)

Abstract

The avian nucleus of the basal optic root (nBOR) is a visual structure involved in the optokinetic response. nBOR consists of several morphologically distinct cell types, and in the present study, we sought to determine if these different cell types had differential projections. Using retrograde tracers, we examined the morphology and distribution of nBOR neurons projecting to the vestibulocerebellum (VbC), inferior olive (IO), dorsal thalamus, the pretectal nucleus lentiformis mesencephali (LM), the contralateral nBOR, the oculomotor complex (OMC) and a group of structures along the midline of the mesencephalon. The retrogradely labeled neurons fell into two broad categories: large neurons, most of which were multipolar rather than fusiform and small neurons, which were either fusiform or multipolar. From injections into the IO, LM, contralateral nBOR, and structures along the midline-mesencephalon small nBOR neurons were labeled. Although there were no differences with respect to the size of the labeled neurons from these injections, there were some differences with the respect to the distribution of labeled neurons and the proportion of multipolar vs. fusiform neurons. From injections into the VbC, the large multipolar cells were labeled throughout nBOR. The only other cases in which these large neurons were labeled were contralateral OMC injections. To investigate if single neurons project to multiple targets we used paired injections of red and green fluorescent retrograde tracers into different targets. Double-labeled neurons were never observed indicating that nBOR neurons do not project to multiple targets. We conclude that individual nBOR neurons have unique projections, which may have differential roles in processing optic flow and controlling the optokinetic response.

Keywords: Optokinetic, Oculomotor, Accessory optic system, Pretectum, Vestibulocerebellum, Inferior olive

Introduction

Self-motion through the environment results in patterns of "optic flow" across the entire retina (Gibson, 1954). Together, nuclei in the pretectum and the accessory optic system (AOS) are involved in the analysis of optic flow (Simpson, 1984; Simpson et al., 1988*b*; Grasse & Cynader, 1990). The pretectum and AOS are highly conserved in vertebrates: the mammalian pretectal nucleus of the optic tract (NOT) is homologous to the nucleus lentiformis mesencephali (LM) in birds, and the avian nucleus of the basal optic root (nBOR) of the AOS is homologous to the medial and lateral terminal nuclei (MTN, LTN) of the mammalian AOS (Simpson, 1984; Fite, 1985; McKenna & Wallman, 1985; Weber, 1985; Simpson et al., 1988*b*; Gamlin, 2005; Giolli et al., 2005).

Address correspondence and reprint requests to: Douglas Wong-Wylie PhD, University of Alberta, Department of Psychology, Edmonton, Alberta, Canada T6G 2E9. E-mail: dwylie@ualberta.ca

Previous reports have shown that neither the LM nor the nBOR can be regarded as homogeneous nuclei, but rather consist of several morphologically distinct cell types (Brecha et al., 1980; Gottlieb & McKenna, 1986; Gamlin & Cohen, 1988; Tang & Wang, 2002; Zayats et al., 2002, 2003). As the analysis of optic flow subserves many functions (Lee & Lishman, 1977; Simpson, 1984; Lappe & Rauschecker, 1994), it is possible that these distinct cell types are specialized with respect to their efferent projections, as well as their function. For example, Prochnow et al. (2007) showed that different cell types in the rat NOT project to the superior colliculus and inferior olive. They also found that these cell types have different physiological properties and are involved in saccades and the slow phase of optokinetic nystagmus, respectively. Recently, we (Pakan et al., 2006) showed that the different efferent projections of LM originate from morphologically distinct types of neurons, and we speculated that they are involved in different components of the optokinetic response or other visual behaviors. Given that LM and nBOR are quite similar with respect to function, response properties, and efferent projections

(McKenna & Wallman, 1985), one might expect that the different cell types in nBOR also have differential projections.

Electrophysiological studies have shown that nBOR neurons have large receptive fields in the contralateral visual field and exhibit direction-selectivity to large-field moving visual stimuli (Burns & Wallman, 1981; Morgan & Frost, 1981; Wylie & Frost, 1990). The nBOR receives primary input from the displaced ganglion cells in the contralateral retina (Karten et al., 1977; Reiner et al., 1979; Fite et al., 1981) and projects to several structures. These include bilateral projections to the medial column of the inferior olive (mcIO), folium IXcd of the vestibulocerebellum (VbC) and the oculomotor complex (OMC), ipsilateral projections to LM and parts of the anterior dorsal thalamus, and a projection to the contralateral nBOR. In addition, the nBOR projects bilaterally to several structures along the midline in the mesencephalon, including the interstitial nucleus of Cajal (IS), nucleus Darkshewitsch (D), the central grey (CtG), and the ventral tegmental area (VTA; Brecha et al., 1980; Wild, 1989; Wylie & Linkenhoker, 1996; Wylie et al., 1997, 1998*b*; Wylie, 2001; Pakan et al., 2006).

nBOR consists of several morphologically distinct cell types (Brecha et al., 1980) with different immunochemical properties (Zayats et al., 2002). However, it is not known if these different neuronal subtypes are associated with different efferent projections. In the present study, using retrograde tracing techniques, we examined differences in the morphology and distribution of nBOR neurons that project to several different targets: VbC, mcIO, LM, OMC, the contralateral nBOR, dorsal thalamus, and structures along the midline of the mesencephalon.

Materials and methods

The methods reported herein conformed to the guidelines established by the Canadian Council on Animal Care and were approved by the Biosciences Animal Care and Policy Committee at the University of Alberta. Silver King and homing pigeons, obtained from various suppliers, were anesthetized with an intramuscular injection of a ketamine (65 mg/kg)/xylazine (9.4 mg/kg) cocktail, and were given supplemental doses as needed to maintain anesthesia. The animals were placed in a stereotaxic device with pigeon ear bars and beak adapter so that the orientation of the skull conformed to the atlas of Karten and Hodos (1967). Sufficient skull and dura were removed to expose the brain surface and allow access to one of the following: the dorsal thalamus, structures along the midline-mesencephalon, VbC, mcIO, OMC, LM, or nBOR. All target sites were localized using a stereotaxic atlas (Karten & Hodos, 1967). For injections into the VbC, mcIO, LM, and nBOR we also relied on single-unit recordings made with glass micropipettes (tip diameters 4–5 μm) filled with 2 M NaCl, which were advanced using an hydraulic microdrive to record the responses of neurons in these structures to optic flow stimuli (e.g., Wylie & Frost, 1990, 1996; Winship & Wylie, 2001; Winship et al., 2005).

Studies using cholera toxin subunit B (CTB) as a retrograde tracer

For injections into the VbC, mcIO, LM, and nBOR, after recording from optic flow sensitive cells, the recording electrode was replaced with a micropipette (tip diameter 20 μm) filled with CTB (low-salt version, Sigma, St. Louis, MO; 1% in 0.1 M phosphate-buffered saline (PBS, pH 7.4)) and the nucleus was located again by isolating cells responsive to large field visual stimuli. For all other target sites (dorsal thalamus and midline structures), injections were made according to the stereotaxic coordinates. In all cases, the CTB was injected iontophoretically for 10–15 min (+4 μamps, 7 s on, 7 s off). Following the injection, the micropipette was left in place for 5 min then removed and the exposures were closed. Once the animal regained consciousness, buprenorphine (2 mg/kg, i.m.) was administered as an analgesic.

After a survival time of 3–5 days, the animals were administered an overdose of sodium pentobarbital (100 mg/kg), and perfused with 0.9% saline followed by 4% paraformaldehyde in 0.1 M phosphate buffer (PB). The brain was extracted from the skull, embedded in gelatin, and placed in 30% sucrose in 0.1 M PB for cryoprotection. Using a microtome, frozen sections in the coronal plane (40 μm thick) were collected, and sections were processed for CTB based on the protocol outlined by Wild et al. (1993; see also Veenman et al., 1992). Sections were initially rinsed in 0.1 M PBS. They were then washed in a 25% methanol, 0.9% hydrogen peroxide solution for 30 min to decrease endogenous peroxidase activity. Sections were rinsed several times in PBS then placed in 4% rabbit serum with 0.4% Triton X-100 in PBS for 30 min. Tissue was subsequently incubated for 20 h in a primary antibody for CTB, goat anti-Choleragenoid (1:20,000; List Biological Laboratories, Campbell, CA) with 0.4% Triton X-100 in PBS. Sections were then rinsed in PBS (several times) and incubated for 60 min in biotinylated rabbit anti-goat antiserum (1:600; Vector Laboratories, Burlingame, CA) with 0.4% Triton X-100 in PBS. Tissue was rinsed several times with PBS and incubated for 90 min in ExtrAvidin (1:1,000; Sigma, St. Louis, MO) with 0.4% Triton X-100 in PBS. Subsequent to a few washes with PBS, the tissue was incubated for 12 min in filtered 0.025% diaminobenzidine (DAB) and 0.006% cobalt chloride in PBS. 0.005% hydrogen peroxide was added to the DAB solution, and the sections were reacted for up to 6 min. The sections were then rinsed several times with PBS, mounted onto gelatin coated slides, lightly counterstained with Neutral Red and cover slipped with Permount.

Double-labeling fluorescent studies

We also performed double-labeling experiments using green and red fluorescent latex microspheres (LumaFluor Corp, Naples, FL) as retrograde tracers. These were pressure injected through a glass micropipette (tip diameter 20 μm), into the mcIO, LM, OMC, dorsal thalamus, VbC, and nBOR, using a Picospritzer II (General Valve Corporation). Viewing through a surgical microscope, we monitored the movement of the meniscus to inject from 0.05 to 0.2 μl. With larger injection volumes, typically used for injection into the cerebellum, the resultant injection sites were about 1 mm in diameter. As with the CTB injections, for injections into LM, VbC, nBOR and mcIO, the nuclei were first localized by recording the responses of neurons to optic flow stimuli. After a recovery period of 2–5 days, the animals were deeply anesthetized with sodium pentobarbital (100 mg/kg) and immediately perfused with heparinized phosphate buffered saline (0.9% NaCl, 1 ml/100 ml heparin, 0.1 M phosphate buffer). The brains were extracted, then flash-frozen in 2-methylbutane and stored at -80°C until sectioned. Brains were embedded in optimal cutting temperature medium and 40 μm coronal sections were cut through the brainstem and cerebellum with a cryostat and mounted on electrostatic slides.

Microscopy

Sections were viewed with a compound light microscope (Leica DMRE) equipped with the appropriate fluorescence filters. The red and green latex microspheres fluoresce under rhodamine and FITC filters, respectively. The CTB-reacted tissue was examined using standard light microscopy and drawings were made with the aid of a drawing tube. Images were obtained using the OPENLAB Imaging system (Improvision, Lexington, MA) and Adobe Photoshop software was used to compensate for brightness and contrast. OPENLAB was also used to measure the size (area) of CTB-labeled neurons.

Nomenclature

Brecha et al. (1980) defined the nBOR complex as consisting of three parts: nBOR proper (nBORp), which comprises the bulk of the nucleus; nBOR dorsalis (nBORd) which is a cap that surrounds the dorsal and caudal margins of nBORp; and nBOR lateralis, which sits atop the stratum opticum (SOp) lateral to the nucleus. McKenna and Wallman (1981) found that nBOR lateralis is continuous with LM, and represents LM's caudo-medial tail. Moreover, they showed that with respect to direction-preference for visual stimuli, lateralis resembles LM rather than nBOR. In dozens of species of birds, Iwaniuk and Wylie (2007) observed in Nissl stained coronal sections that lateralis is continuous with LM. Also, the unique connections of nBOR, the contralateral nBOR and the OMC, do not involve lateralis. For these reasons, we consider nBOR lateralis as part of LM rather than the nBOR complex.

Results

Data are described from experiments performed on 33 pigeons (Table 1). Twenty-one pigeons were used for the retrograde studies using CTB injected into a single target site. The CTB cases included unilateral injections in the VbC ($n = 5$) IO ($n = 3$), contralateral nBOR ($n = 3$), dorsal thalamus ($n = 3$), LM ($n = 3$), and OMC ($n = 1$). In addition, there were three cases, two unilateral, and one bilateral that were grouped together as "midline-mesencephalon." The other 12 birds received injections of red or green LumaFluors in different efferent targets of the nBOR. From both the CTB and LumaFluor injections, we observed differences in the size, morphology, and distribution of neurons associated with the different projection sites. In our descriptions of morphology and quantification of neuron size, we relied only on the CTB cases, as this tracer results in uniform and complete labeling of the entire soma and proximal dendrites. Photomicrographs of representative retrograde labeling from the CTB experiments are shown in Figs. 1 and 2, and from the LumaFluor experiments in Fig. 3. Drawings of coronal sections through the nBOR illustrating the distribution of labeled cells from various injections are shown in Figs. 6 and 7.

VBC-projecting nBOR neurons

Previous studies using anterograde techniques have shown that the projection from nBOR to the VbC is bilateral and terminates in the granule layer as mossy fiber rosettes (Brecha et al., 1980). We directed our injections to folium IXcd. The complex spike activity of Purkinje cells in folium IXcd responds to patterns of optic flow resulting from either self-translation or self-rotation (Wylie & Frost, 1991, 1993, 1999*b*; Wylie et al., 1993, 1998*a*). Once responsive neurons were found, we made the injection in the adjacent granule cell layer. Spread of the injection site to other folia was not a concern because folium X does not receive direct input from nBOR (Brecha et al., 1980; Wylie & Linkenhoker, 1996; Wylie et al., 1997), although the nBOR does project to folia VI-IXab, retrograde studies show that the magnitude of this pro-

Table 1. *Retrograde tracer injection sites and fluorescent cell count*

CTB Injections

Case	Target	Case	Target	Case	Target
VbC#1	VbC	IO#1	IO	DTHAL#1	dorsal thalamus
VbC#2	VbC	IO#2	IO	DTHAL#2	dorsal thalamus
VbC#3	VbC	IO#3	IO	DTHAL#3	dorsal thalamus
VBC#4	VbC	c-nBOR#1	nBOR	LM#1	LM
VBC#5	VbC	c-nBOR#2	nBOR	LM#2	LM
OMC	OMC	c-nBOR#3	nBOR	LM#3	LM
MID-MES#1	Midline-Mesencephalon	MID-MES#2	Midline-Mesencephalon	MID-MES#3	Midline-Mesencephalon

LumaFluor Injections

Case	Target-green	# green cells	Target-Red	# red cells	#double-labeled
DTHAL-IO	dorsal thalamus	73	ipsi-IO	10	0
DTHAL-LM	dorsal thalamus	223	LM	888	0
IO-LM#1	ipsi-IO	60	LM	224	0
IO-LM#2	LM	370	contra-IO	168	0
nBOR-DTHAL	nBOR	186	dorsal thalamus	202	0
nBOR-IO#1	nBOR	184	contra-IO	78	0
nBOR-IO#2	nBOR	592	ipsi-IO	136	0
nBOR-LM	nBOR	370	LM	624	0
nBOR-VbC	nBOR	756	VbC	432	0
OMC-VbC	OMC	363	VbC	80	0
VbC-IO#1	VbC	73	IO	380	0
VbC-IO#2	VbC	738	IO	269	0

jection is very small compared to the projection to IXcd (Brecha et al., 1980; Pakan & Wylie, 2006).

There were nine cases in which the VbC was injected unilaterally; five CTB cases, and four LumaFluor cases. From these injections, large neurons (330.2 ± 16.9 μm^2; mean ± s.e.m.) were invariably labeled (Figs. 1E, 1F, 3F). The majority (85%) of these neurons was multipolar (Fig. 4) and they were distributed uniformly throughout nBOR (Figs. 1E, 6B).

IO-projecting nBOR neurons

For the IO, the injections were aimed at the optic flow responsive regions in the medial column (mcIO; Winship & Wylie, 2001). The projection from the nBOR is heavier to the rostral, as opposed to the caudal, region of mcIO. To access the mcIO, the electrode had to pass through the cerebellum, thus we were careful to ensure that there was no leakage of the tracer in this regard.

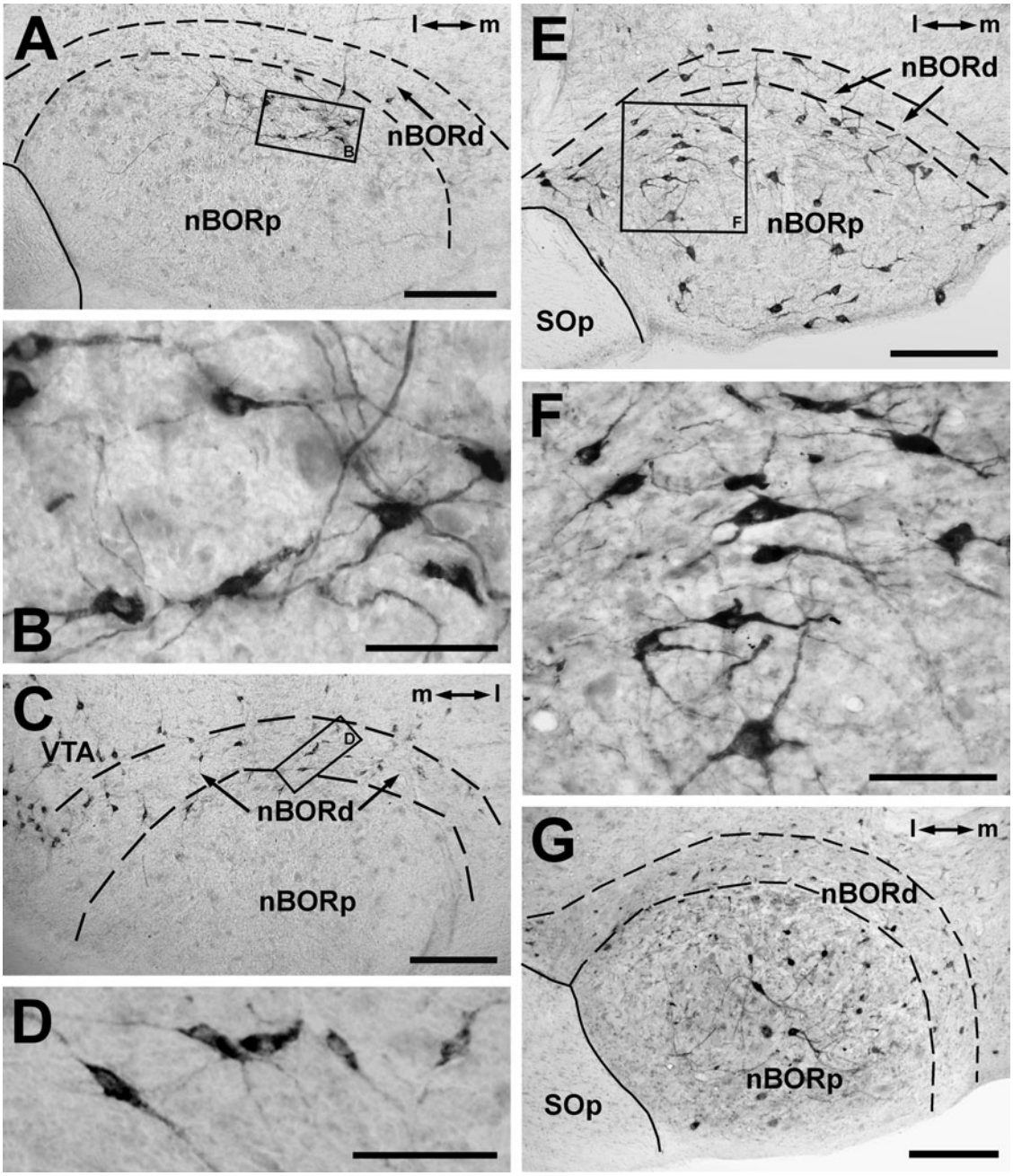

Fig. 1. Photomicrographs of coronal sections through the nucleus of the basal optic root (nBOR), showing retrogradely labeled neurons from injections of cholera toxin subunit B into the inferior olive (IO; **A–D**; case IO#1), vestibulocerebellum (VbC; **E**, **F**; case VbC#5), and oculomotor complex (OMC; **G**; case OMC). Injections in the IO labeled a cluster of small cells dorsally in the contralateral nBOR (**A**, **B**) and a more diffuse group spanning nBOR dorsalis (nBORd) and the ventral tegmental area (VTA) on the ipsilateral side (**C**, **D**). Injections into the VbC labeled very large multipolar cells throughout nBOR bilaterally (**E**, **F**). Such large cells were also seen from injections into the contralateral OMC (**F**), m, medial; l, lateral. Stratum opticum (SOp). Scale bars: 200 μm in **A**, **C**, **E**, and **G**; 100 μm in **G**; 75 μm in **F**; 50 μm in **B** and **D**.

The IO was injected in three of the CTB cases and seven of the LumaFluor cases. Small neurons were labelled bilaterally in the nBOR (ipsi, 132.6 ± 6.4 μm^2; contra 131.7 ± 4.6 μm^2; mean ± s.e.m.). Neurons that were multipolar and fusiform/ovoid were equally represented (Figs. 1B, 1D, 4). In the contralateral nBOR, the neurons were found in a circumscribed region in the dorsal part of nBORp and encroaching on the adjacent nBORd (Figs. 1A, 6A). In the ipsilateral nBOR, the neurons were more widely distributed and found mainly in nBORd and adjacent regions of the nBORp and VTA (Figs. 1C, 6A). The IO-projecting neurons in the ipsilateral nBOR were located more caudally than those in the contralateral nBOR (Fig. 6A; see below).

LM-Projecting nBOR neurons

The heaviest projection of the nBOR is to the ipsilateral LM. This projection spans the rostro-caudal and dorso-ventral extent of the medial and lateral subnuclei of LM (Wylie et al., 1997). The LM was injected in three of the CTB cases and four of the LumaFluor cases. Critically, none of these injections spread into the dorsal thalamus. Small cells were labeled from these injections (106.0 ± 6.2 μm^2; mean ± s.e.m.), most of which were fusiform/ovoid (85%) as opposed to multipolar (Figs. 2E, 3C, 4). Neurons were found in both nBORp and nBORd and also dorsal to the complex itself (Figs. 3C, 3D, 7A–7C).

Dorsal thalamus-projecting nBOR neurons

Wylie et al. (1998*b*) showed that the projection from the nBOR to the thalamus is directed mainly to the lateral subnucleus of the ipsilateral anterior dorsolateral thalamus (DLL). This is one component of the principal optic nucleus of the thalamus and is considered the homolog of the mammalian dorsal lateral geniculate nucleus (dLGN; Karten et al., 1973; Shimizu & Karten, 1991). For

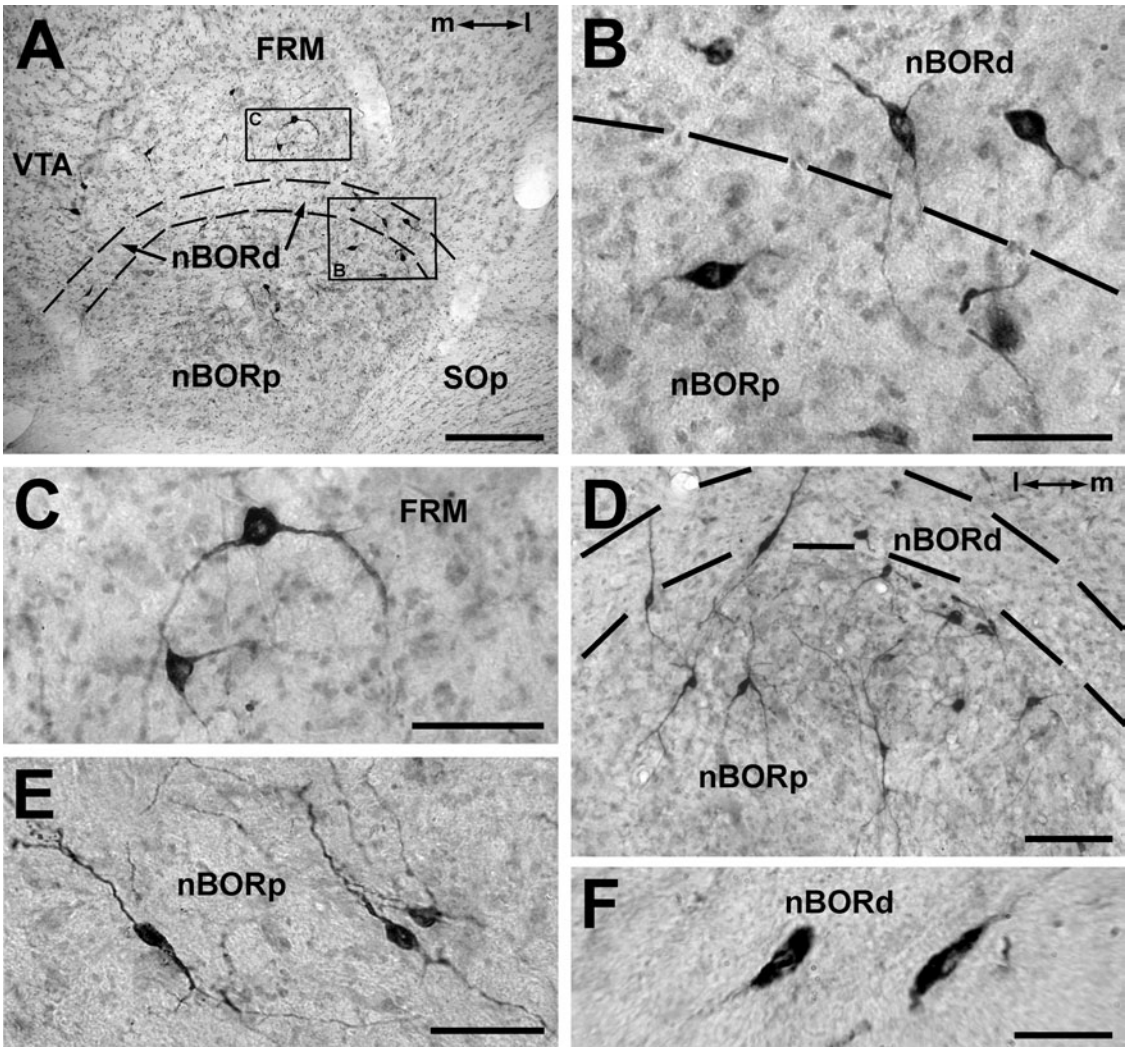

Fig. 2. Photomicrographs of coronal sections through the nucleus of the basal optic root (nBOR) showing small neurons labeled with cholera toxin subunit B. **A–C** show cells labeled from injections in the contra nBOR (case C-NBOR#1). The rectangles in **A** indicate the areas shown in **B** and **C**. Most cells were found in nBOR dorsalis (nBORd) and the dorsal part of nBOR proper (nBORp) (**B**), and some were dorsal to the nBOR complex in the medial mesencephalic reticular formation (FRM) (**C**). **D**, **E**, and **F**, respectively show cells retrogradely labeled from injections in the midline-mesencephalon (case MID-MES#3), lentiformis mesencephali (LM; case LM#3), and the dorsal thalamus (case DTHAL#1). m, medial; l, lateral. Stratum opticum (SOp). Scale bars: 200 μm in **A**; 100 μm in **D**; 50 μm in **B**, **C**, **E**; 10 μm in **F**.

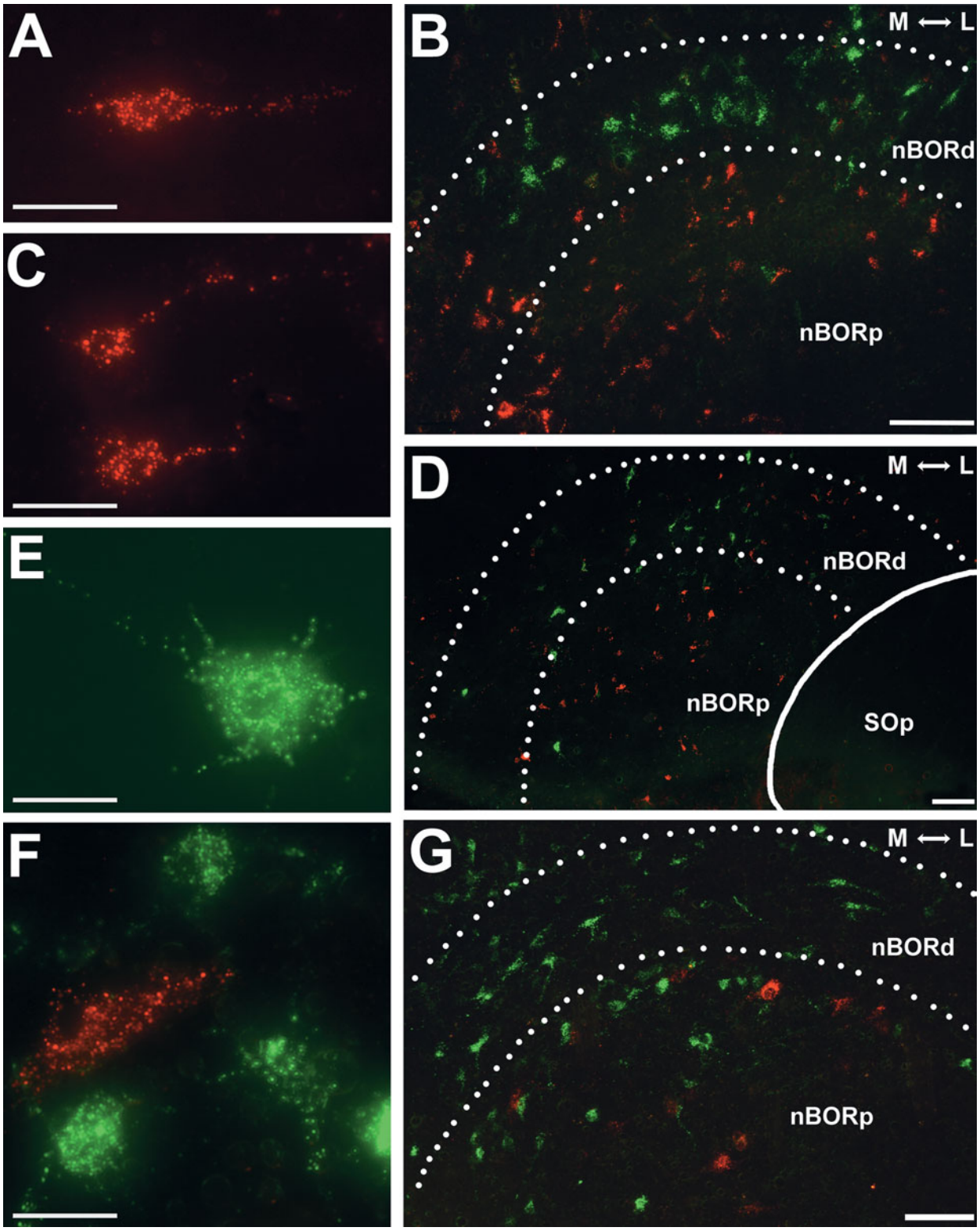

Fig. 3. Photomicrographs of coronal sections through the nucleus of the basal optic root (nBOR) showing cells labeled with fluorescent microspheres. (**A**) Shows a cell labeled from an injection in the inferior olive (IO; case LMIO2). (**B** and **C**) Show cells labeled from case DTHAL-LM in which green LumaFluor was injected in the dorsal thalamus and red was injected in the pretectal nucleus lentiformis mesencephali (LM). (**D**) Shows labeled cells from case nBOR-LM, in which red was injected in the ipsilateral LM and green was injected in the contralateral nBOR. (**E**) Shows a cell labeled from an injection in the vestibulocerebellum (VbC; case VbC-IO#1) and (**F** and **G**) Show cells labeled from case OMC-VbC in which green was injected in the oculomotor complex (OMC) and red was injected in the VbC. The cells labeled from the LM injections were found in nBOR proper (nBORp) and dorsally (nBORd) whereas cells labeled from contra-nBOR and dorsal thalamus injections were found mostly in nBORd. Note the large cells labeled from the VbC and OMC injections (**E**, **F**). Scale bars: 25 μm in **A**, **C**, **E**, **F**; 100 μm in **B**, **D**, **G**.

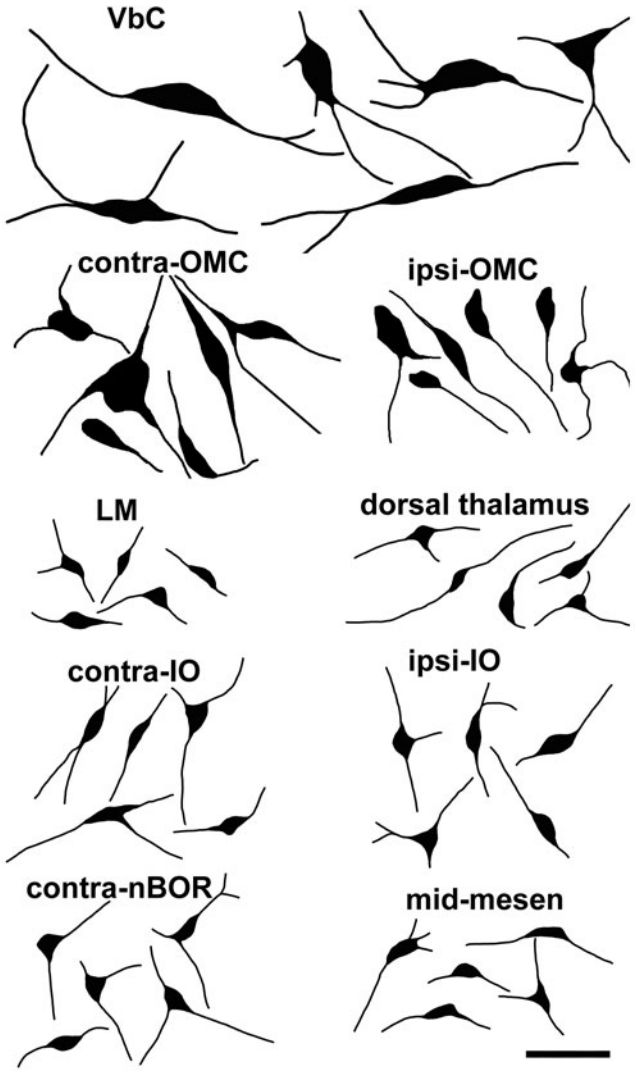

Fig. 4. A comparison of the morphology and size of neurons in the nucleus of the basal optic root (nBOR) that project to the vestibulocerebellum (VbC), the ipsi- and contralateral oculomotor complex (ipsi-, contra-OMC), the nucleus lentiformis mesencephali (LM), the dorsal thalamus, the ipsi- and contralateral inferior olive (ipsi-, contra-IO), the contralteral nBOR (contra-nBOR) and the midline-mesencephalon (mid-mesen). Silhouettes of CTB-labeled neurons have been drawn to the same scale. The VbC- and OMC-projecting neurons were much larger than the others and they tend to be multipolar rather than fusiform. Scale bar = 50 μm.

these injections, we were careful to ensure that they did not encroach ventrolaterally on LM.

The dorsal thalamus was injected in three CTB cases and three of the LumaFluor cases. Like those labeled from injections in the LM, the dorsal thalamic-projecting nBOR neurons were small ($123.4 \pm 7.8\ \mu m^2$; mean ± s.e.m.), and the majority were fusiform/ovoid (85%) as opposed to multipolar (Figs. 2F, 3B, 4). These neurons were distributed mainly in nBORd and dorsal to the border of the nBOR complex (Figs. 7B, 7D).

Contralateral nBOR-projecting nBOR neurons

The nBOR projects to the contralateral nBOR and anterograde studies have shown that the projection is mainly to the dorsal parts of the nBOR complex (Brecha et al., 1980; Wylie et al., 1997). The nBOR was injected in three of the CTB cases and five of the LumaFluor cases. From these injections, small neurons ($124.1 \pm 7.3\ \mu m^2$; mean ± s.e.m.) were labeled in the contralateral nBOR (Figs. 2B, 2C). Multipolar and fusiform/ovoid cells were found in equal proportions, and most labeled cells were located in nBORd, dorsal nBORp, and some were located dorsal to the nBOR complex in VTA and medial mesencephalic reticular formation (FRM; Figs. 2A, 3D, 7A, 7D).

nBOR neurons projecting to the midline-mesencephalon

Previous studies have shown that nBOR projects heavily to the accessory optic nuclei (AON), a group of structures lying on the midline of the mesencephalon that includes IS and D (Brecha et al., 1980). In an anterograde study, Wylie et al. (1997) showed that fibers exit the nBOR medially, travel dorsally to the AON and collateralize heavily to adjacent structures including VTA, the red nucleus (Ru), the stratum cellulare externum/internum and CtG. Injecting these small individual nuclei in this region is extremely difficult, and because individual fibers collateralize throughout this region, we considered this area as a group. There were three cases in which CTB was injected along the midline-mesencephalon. In case MID-MES#1, the injection was unilateral, and included IS, D, the medial Ru, VTA, SCE and the caudal part of Campi Foreli (CF). In case MID-MES#2, the injection was centered on the midline and was largely confined to the VTA bilaterally, with some spread to Ru, IS, CF, and SCE. In case MID-MES#3, the injection was unilateral and centered on the lateral Ru with spread to the adjacent FRM, IS, CF, and SCE. The morphology, size, and distribution of the retrograde labeled cells in the nBOR were not appreciably different from these three cases. Cells were found bilaterally in nBOR and were small ($132.9 \pm 8.3\ \mu m^2$; mean ± s.e.m.). Most were fusiform/ovoid (70%) as opposed to multipolar (30%) (Fig. 2D). With respect to distribution, the labeling was found dorsally in the nBORp, nBORd, and dorsal to the nBOR complex (Figs. 2D, 6C).

OMC-projecting nBOR neurons

We had two OMC cases: one CTB injection (case OMC), and one LumaFluor injection (case OMC-VbC). For the CTB case, the injection was largely unilateral, and included the dorsomedial, dorsolateral, and ventromedial subdivisions of the oculomotor nucleus, as well as the Edinger-Westphal nucleus. There was spread to the adjacent CtG, the medial longitudinal fasciculus, the vestibular-mesencephalic tract, the brachium conjuctivum, and diffuse spread rostrally into midline-mesencephalon structures, including IS, D, and Ru. Retrograde labeled cells were observed in the lateral subnucleus of LM, consistent with an injection in the midline-mesencephalon (Pakan et al., 2006). As the LM does not project to the OMC, we must conclude that the injection spread to the midline-mesencephalon. Although the injection appeared to be unilateral, there were some labeled fibers in the contralateral oculomotor nerve. Most of these fibers were located medially and although these are likely innervating the contralateral superior rectus, it is possible that some of this labeling was due to spread across the midline. Also there were retrograde labeled neurons in the contralateral LM and PPC, indicative of spread across the midline. Thus, it appears that although the injection was largely unilateral, there was some spread across the midline. In the LumaFluor case (OMC-VbC), the injection was bilateral, and centered on the ventromedial subdivision of the oculomotor nucleus. The injection spread into the

dorsomedial and dorsolateral subnuclei, but the Edinger-Westphal nucleus was largely spared. There was spread ventrally into the parts to the brachium conjuctivum, and rostrally into the midline-mesencephalic structures of the AON including IS, D, CtG, SCE, and Ru. As with the CTB case, there was retrograde labeling in the LM and PPC. As such, both injections included the OMC and the midline-mesencephalon. The retrograde labeled cells in nBOR from these injections were quite variable in size (65–805 μm^2 as measured from the CTB case) and included small and large neurons (Figs. 1G, 3E, 3F). Those in the contralateral nBOR were larger on average than those in the ipsilateral nBOR (contra, 258.7 $\pm$ 12.9 μm^2; ipsi, 180.5 $\pm$ 9.2 μm^2, mean $\pm$ s.e.m.).The large neurons found in the contralateral nBOR were as large as those retrograde labeled from the VbC (Figs. 3F, 5). Neurons were found in nBORd and nBORp, with a dorsal emphasis, as expected from the spread of the injections to the midline-mesencephalon.

A Comparison of the size of nBOR neurons

Fig. 4 shows the silhouettes of nBOR neurons projecting to VbC, the contra- and ipsilateral OMC, LM, dorsal thalamus, the contra- and ipsilateral IO, contralateral nBOR, and the midline-mesencephalon all drawn to the same scale. The OMC-projecting neurons, drawn from the CTB case represent midline-mesencephalon projecting cells as well. Nonetheless, we purposefully selected cells from nBORp as opposed to nBORd from this case, because labeling from the midline-mesencephalon was heavily biased to the nBORd. Thus, the cells we selected are more likely to represent OMC-projecting neurons. Clearly, the VbC-projecting neurons were much larger than the others. From among the other groups, cells of this size were only seen from the contra-OMC projecting cells. The cells projecting to the contralateral nBOR, dorsal thalamus, IO, LM, and midline-mesencephalon were all very similar in size. The only noticeable difference was that cells with a fusiform/ovoid as opposed to a multipolar profile were more prevalent among the LM-, dorsal thalamic- and midline-mesencephalic-projecting neurons. To quantitatively examine the size of neurons, we used a one-way ANOVA with injection site as a grouping factor and compared all groups with Tukey's HSD tests. We subjected the data to an ln-transform to normalize the distributions. Fig. 5 shows box plots of these data. There was a significant effect of group ($F(8,577) = 48.9$; $p < 0.0001$) and planned comparisons revealed

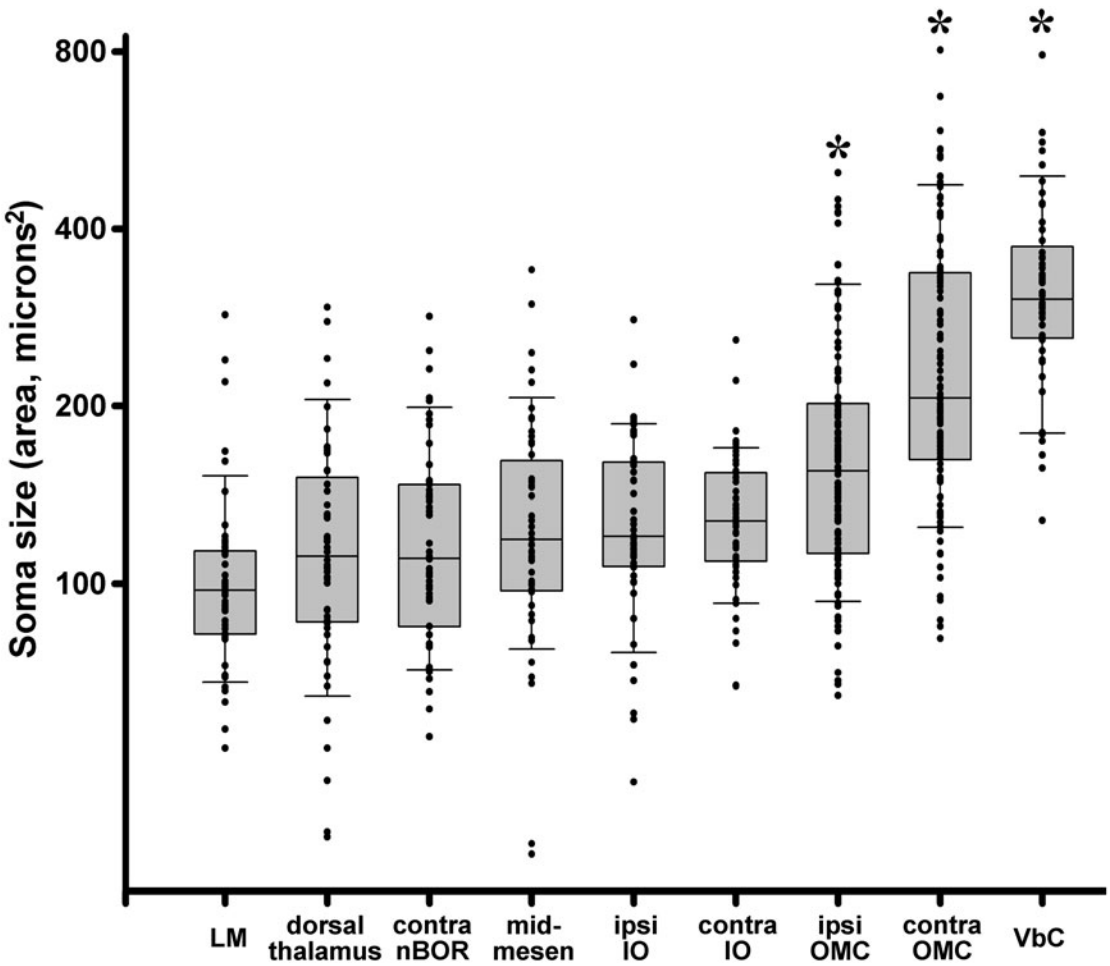

Fig. 5. A comparison of the sizes of neurons in nucleus of the basal optic root (nBOR). Box plots show the cross-sectional areas of nBOR cells retrograde labeled from injections into the nucleus lentiformis mesencephali (LM), dorsal thalamus, midline-mesencephalon (mid-mesen), contralateral nBOR, contra- and ipsilateral inferior olive (IO), contra- and ipsilateral oculomotor complex (OMC) and the vestibulocerebellum (VbC). Note that the data has been subjected to an ln transform. The asterisks (*) indicate the ipsi-OMC, contra-OMC and VbC groups were statistically different from all other groups and each other (Tukey HSD, $p < .05$).

that the VbC, contra-OMC and ipsi-OMC neurons were larger than all other groups and different from each other (Tukey HSD; α set to 0.05).

Double-labeling fluorescent studies

There were 12 cases in which red and green LumaFluors were injected into two projection sites of the nBOR. The CTB experiments showed that small neurons in the nBOR project to the LM, contralateral nBOR, IO, dorsal thalamus, and the midline-mesencephalon. Many of the retrograde neurons from injections in these structures were found dorsally in the nBOR complex. The purpose of the double-labeling fluorescent experiments was (1) to determine if any individual nBOR neurons project to multiple sites, as evidenced by double-labeled neurons and (2) to directly compare the distributions of neurons labeled from different projection sites. Table 1 lists the injection sites for all 12 experiments, as well as the number of retrograde labeled cells examined from each injection. In none of these experiments were double-labeled neurons observed. That is, despite the fact that small neurons project to the LM, contralateral nBOR, IO, and dorsal thalamus, individual neurons do not project to more than one of these sites (Figs. 3B, 3D). Moreover, in case OMC-VBC, large neurons labeled from injections in both the VbC and OMC were intermingled in the nBOR, but no double-labeled neurons were found (Figs. 3E–3G). The distributions of labeled neurons from the injections were consistent with those observed from the CTB cases. Data from four cases are shown in Fig. 7. In Figs. 3A–3C, injections in the LM were combined with injections in the contralateral nBOR (A), ipsilateral IO (B), and dorsal thalamus (C). From the LM injections, there was consistent labeling in nBORp and nBORd, whereas from the other injections the labeling was concentrated in nBORd and dorsal to the nBOR complex. Note that the cells labeled from injection into LM and the other sites were intermingled in these dorsal regions.

Differences in the rostro-caudal distribution of labeled cells

From some of the injections there was labeling that consistently appeared biased toward the rostral or caudal end of nBOR. From injections in the IO, labeling in the contralateral nBOR was rostral to that in the ipsilateral nBOR (Figs. 6A, 7C). From injections into the contralateral nBOR, labeling was heavier in the caudal nBOR (Figs. 7A, 7D). To illustrate these observations, using data from both the CTB and LumaFluor cases, we divided the nBOR into six equal rostro-caudal increments, counted the number of neurons within each interval, and normalized the resultant distribution for each case. Finally we averaged cases for each injection site (LM, VbC, contra-nBOR, ipsi-IO, contra-IO, ipsi-OMC, contra-OMC, dorsal thalamus, and midline-mesencephalon). In Fig. 8, we show the rostro-caudal distribution of cells labeled from injections in the ipsi-IO, contra-IO and contra-nBOR. All other groups, which showed no obvious bias in the rostro-caudal distribution, are grouped together.

Discussion

Previous studies have shown that nBOR neurons exhibit direction-selectivity to large field stimuli moving in the contralateral visual field (Burns & Wallman, 1981; Morgan & Frost, 1981; Gioanni et al., 1984; Wylie & Frost, 1990). The nBOR and medial and lateral terminal nuclei in mammals, have been linked to the analysis of optic flow in general, and the generation of the optokinetic response (OKR) in particular (Fite et al., 1977; Gioanni et al., 1983; Simpson, 1984). Previous neuroanatomical studies have indicated that nBOR is not homogeneous, but consists of several different cell types (Brecha et al., 1980; Zayats et al., 2002). In pigeons, Brecha et al. (1980) described three different cell types: large ($\approx$500 μm^2) stellate cells, medium-sized ($\approx$300 μm^2) ovoid cells and small ($\approx$150 μm^2) spindle-shaped cells. In chickens, Zayats et al. (2002) described large ($\approx$1000 μm^2) neurons which were multipolar or fusiform, medium-sized ($\approx$500 μm^2) multipolar neurons, and small (100–150 μm^2) neurons that were fusiform or multipolar. In the present study, with injections of retrograde tracers into these projections sites, we showed that different projections are associated with differences in morphology and distribution of retrograde labeled neurons in nBOR. Moreover, with double-labeling studies, we showed that neurons are associated with a single projection, and do not collateralize to multiple sites. In a study of the rat MTN, Clarke et al. (1989) came to the same conclusion. Using double-labeling retrograde techniques, they found that over 97% of MTN neurons were single-labeled after injections of retrograde tracers into different projection sites (see also Schmidt et al., 1998). This is not to say that axons of nBOR neurons never collateralize. Anterograde studies have shown that axons of nBOR neurons do collateralize locally. For example, axons originating in the nBOR and projecting to the midline mesencephalon generally collateralize to several structures in the area: IS, D, CtG, SCE (Wylie et al., 1997). Likewise, some mossy fibers projecting to the VbC give collaterals to the cerebellar nuclei and, although quite rare, the vestibular nuclei (Wylie & Linkenhoker, 1996). Finally, a few of the IO-projecting axons give collaterals to the pontine nuclei en route.

The LM, which is homologous to the mammalian NOT, can be considered a sister nucleus to nBOR for several reasons. Like nBOR, LM neurons exhibit direction-selectivity to large field stimuli moving in the contralateral visual field (Winterson & Brauth, 1985; Wylie & Frost, 1996; Wylie & Crowder, 2000) and are involved in the generation of the OKR (for review see McKenna & Wallman, 1981, 1985; Simpson et al., 1988*a*). LM has many of the same efferent projections as nBOR, including the VbC, IO, dorsal thalamus, nBOR, and the midline-mesencephalon (Clarke, 1977; Azevedo et al., 1983; Gamlin & Cohen, 1988; Wild, 1989). LM also consists of morphologically distinct cell types (Zayats et al., 2003) and, similar to the present study, Pakan et al. (2006) showed that different efferent projections of LM arise from different cell types. In this discussion, we will describe each efferent projection of nBOR considering previous studies of the nBOR, comparative data, and the projection from LM.

Projection to the VbC

The nBOR projects to the cerebellum as mossy fibers that terminate in the granular layer in the posterior lobe. This projection is directed mainly to folium IXcd of the VbC, but excludes folium X. Folia VI-IXab also receive input from nBOR but, comparatively, this projection is sparse (Brecha et al., 1980; Pakan & Wylie, 2006). The lateral subnucleus of LM projects mainly to IXcd, whereas the medial subnucleus projects mainly to folia VI-VIII (Pakan & Wylie, 2006). Retrograde labeling studies have shown that large neurons throughout LM, most of which are multipolar, are labeled from injections in the cerebellum (Gamlin & Cohen, 1988; Pakan et al., 2006). These large LM neurons are not labeled from injections into

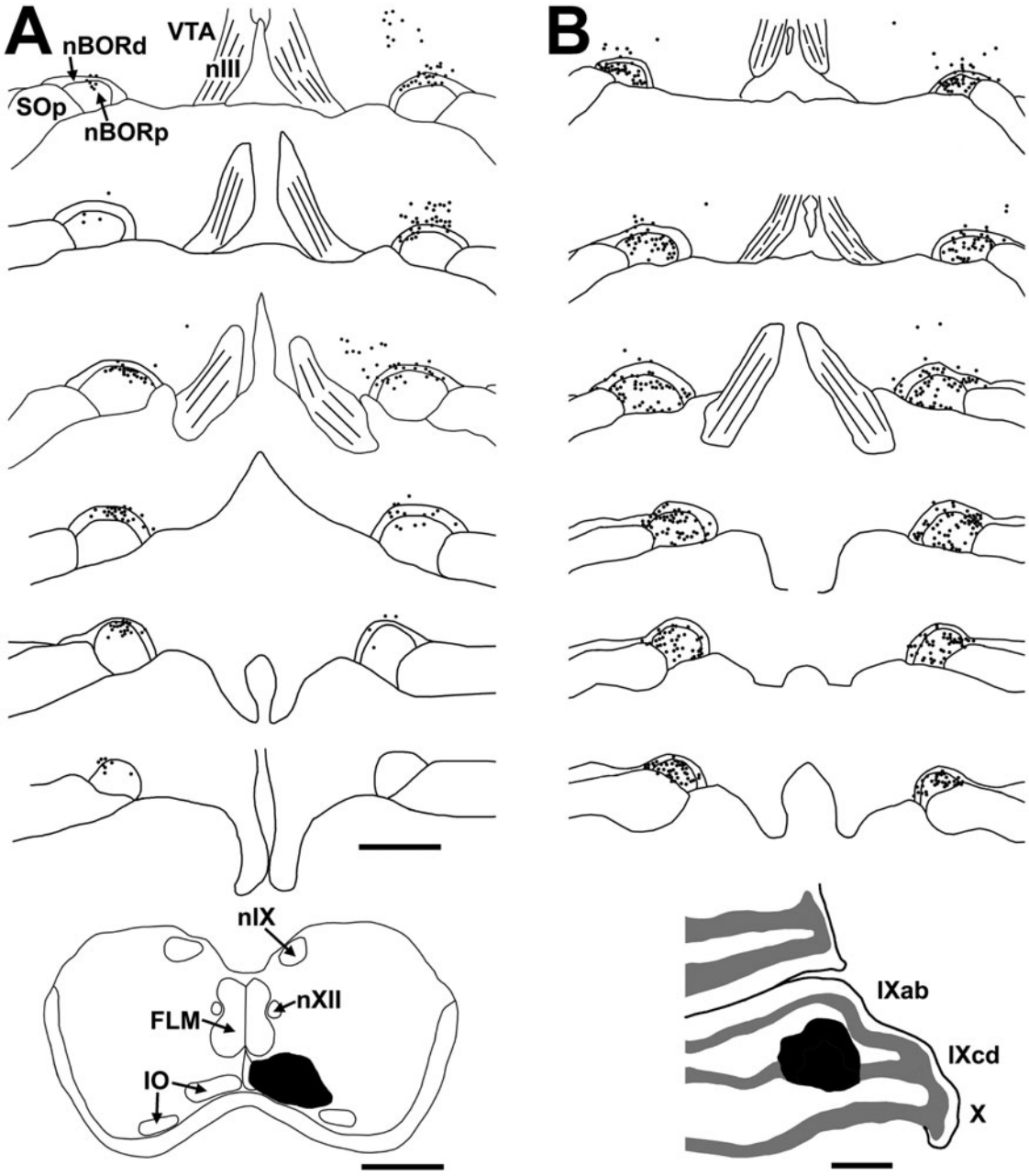

Fig. 6. Distribution of retrograde labeling in the nucleus of the basal optic root (nBOR) from injections of cholera toxin subunit B into the inferior olive (IO; **A**), vestibuolocereblum (VbC; **B**), the midline mesencephalon (**C**), and the oculomotor complex (OMC; **D**). Six coronal sections, at about 200–250 μm intervals, through the nBOR are shown from caudal (top) to rostral. The injection sites are shown in the bottom row. Stratum opticum (SOp), ventral tegmental area (VTA), oculomotor nerve (nIII), nucleus of the hypoglossal nerve (nXII), nucleus of the glossopharyngeal nerve (nIX), medial longitudinal fasciculus (FLM). Scale bars = 1 mm.

other targets of LM (Pakan et al., 2006). In the present study, we found that large, generally mulitpolar neurons throughout nBOR were labeled from cerebellar injections. These likely correspond to the large and medium sized cells described by Zayats et al. (2002). Our findings are consistent with Brecha et al. (1980) who reported that large and medium-sized nBOR cells project to the cerebellum. With respect to morphology and size, the VbC-projecting LM cells are quite similar to the VbC-projecting nBOR cells.

These mossy fiber projections are not found in all vertebrates. In turtles, an nBOR-cerebellar pathway has also been reported, arising from medium and large neurons, but not small neurons (Reiner & Karten, 1978). In fish, mossy fiber pathways to the cerebellum, originating in the homologs of nBOR and LM, have also been described (Finger & Karten, 1978). However, these pathways are not found in frogs (Montgomery et al., 1981). Finally, projections from the lateral and medial terminal nuclei (LTN, MTN) of the AOS have been found in some mammalian species (chinchilla: Winfield et al., 1978; tree shrew: Haines & Sowa, 1985) but not others (cats: Kawasaki & Sato, 1980; rats and rabbits: Giolli et al., 1984, 1985, 1988).

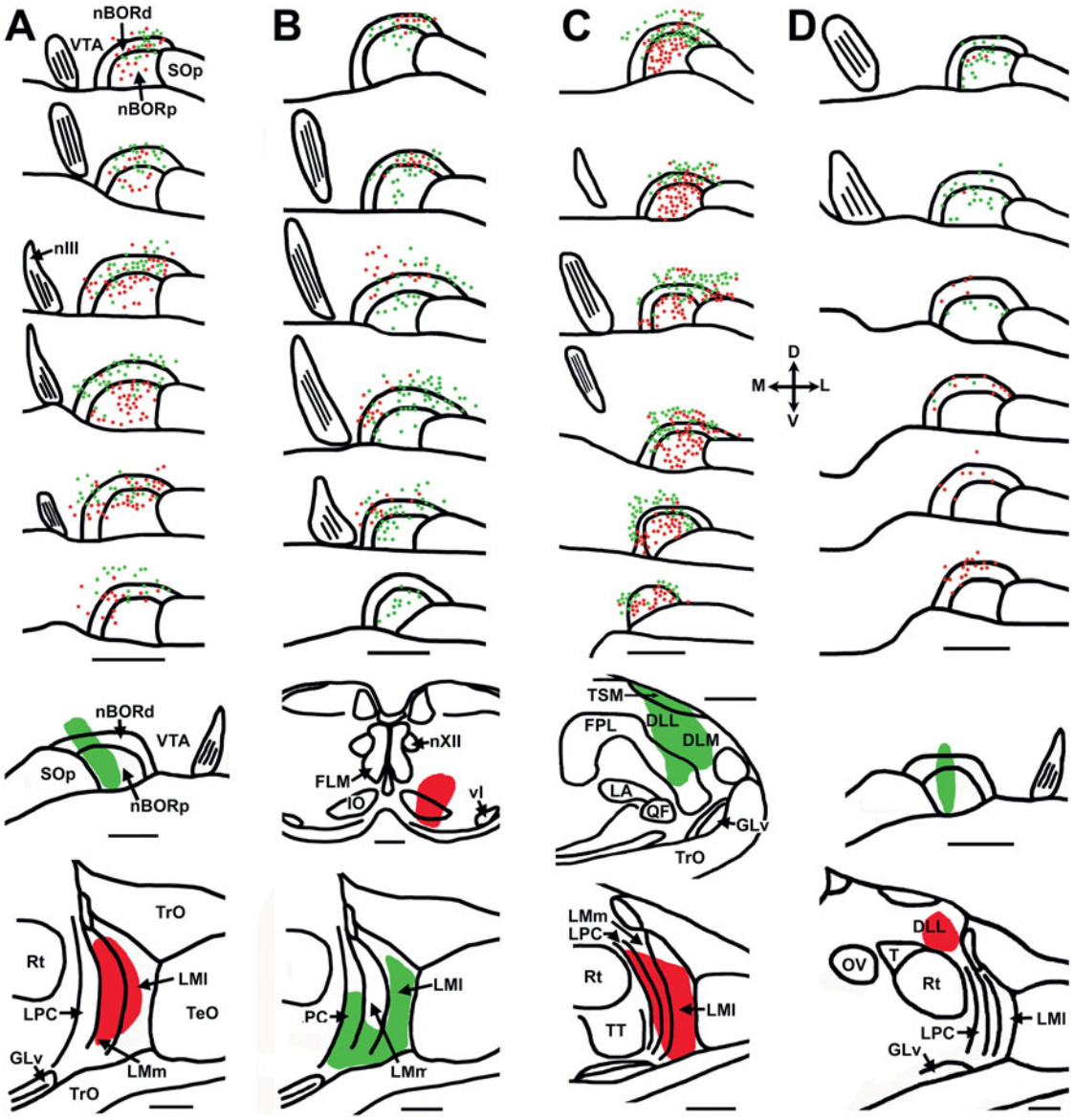

Fig. 7. Distribution of retrograde labeling in the nucleus of the basal optic root (nBOR) from injections of red and green LumaFluors into the pretectal nucleus lentiformis mesencephali (LM; **A**, **B**, **C**), contralateral nBOR (**A**, **D**), dorsal thalamus (**B**, **D**) and the inferior olive (IO; **C**). Six coronal sections, at about 200–250 μm intervals, through the nBOR are shown from caudal (top) to rostral. The injection sites are shown in the two bottom rows. Stratum opticum (SOp), ventral tegmental area (VTA), oculomotor nerve (nIII), nucleus of the hypoglossal nerve (nXII), ventral lamella of the inferior olive (vl), medial longitudinal fasciculus (FLM), tractus opticus (TrO), nucleus laminaris precommissuralis (LPC), nucleus rotundus (Rt), ventral leaflet of the lateral geniculate nucleus (GLv), optic tectum (TeO), nucleus lentiformis mesencephali (medial/lateral subnucleus) (LM(m/l)), anterior dorsolateral thalamus, medial subnucleus (DLM), anterior dorsolateral thalamus, lateral subnucleus (DLL), lateral prosencephalic fasiculus (FPL), tractus septomesencephalicus (TSM), tractus quintofrontalis (QF), nucleus laminaris (La), nucleus triangularis (T), nucleus ovoidalis (OV), tectothalamic tract (TT). Scale bars = 1 mm.

Projection to the OMC

The only other injection target that resulted in labeling of large nBOR neurons was the OMC. Large neurons were clearly labeled in the contralateral nBOR and these resembled those labeled from VbC injections in both size and morphology. The distribution of the VbC-projecting neurons was somewhat broader than the OMC-projecting neurons (Fig. 6B versus 6D). In the double-labeling case (OMC-VbC) no double-labeled neurons were found in nBOR. Thus, the large nBOR neurons projecting to the VbC do not also project to the OMC. Our statistical analysis suggested that the VbC-projecting neurons are larger than the contra-OMC projecting neurons (Fig. 5), however, the OMC injection spread to the midline-mesencephalon, which invariably resulted in the labeling of small cells in nBOR. Brecha et al. (1980) reported that the projection to the ipsilateral OMC originated in small neurons in nBORd. Again noting the caution that our injections spread to the midline-mesencephalon, generally we confirmed these results: neu-

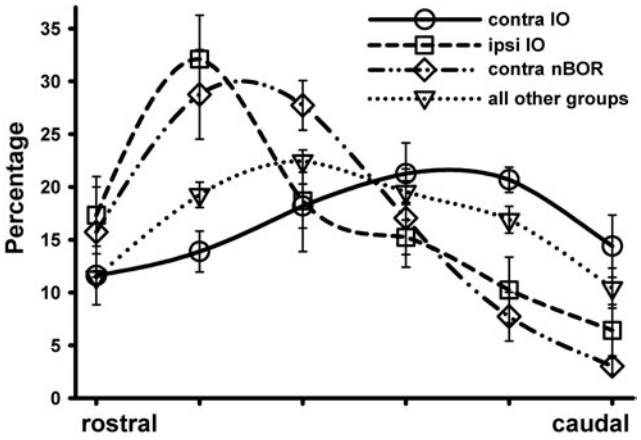

Fig. 8. A quantitative comparison of the rostro-caudal distribution of neurons in the nucleus of the basal optic root (nBOR). The nBOR was divided into six rostro-caudal intervals and the percentage of neurons in each region was calculated for each case. Relative to other groups, (i.e., neurons labeled from injections in the vestibulocerebellum, oculomotor complex, dorsal thalamus, lentiformis mesencephali, and midline-mesencephalon), neurons labeled from injections in the ipsilateral inferior olive (ipsi-IO) and contralateral nBOR (contra-nBOR) were concentrated caudally in the nBOR. The distribution of neurons labeled from injections in the contralateral IO (contra-IO) was skewed slightly rostrally.

rons in the contralateral nBOR were significantly larger than those in the ipsilateral nBOR (Figs. 4, 5) and those in the ipsilateral nBOR were generally found dorsally (Fig. 6D). Labandeira-Garcia et al. (1989) also noted that, from injections in the OMC, neurons in the contralateral nBOR were larger than those in the ipsilateral nBOR. Using anterograde tracing, Brecha et al. (1980) showed that the nBOR projection to the contralateral OMC is directed to the dorsolateral subdivision, whereas that to the ipsilateral OMC was directed to the ipsilateral OMC. However, Wylie et al. (1997) noted projections to the dorsomedial, dorsolateral, and ventromedial subnuclei of the contralateral OMC, and the dorsolateral and ventromedial subnuclei of the ipsilateral OMC. They also reconstructed individual axons and showed that individual fibers originating in the nBOR could innervate all subdivisions of the oculomotor nucleus.

Projection to the IO

The bilateral projection from the nBOR to IO is directed to the medial column (mcIO) (Brecha et al., 1980; Wylie et al., 1997). The mcIO in turn projects to the contralateral VbC, terminating as climbing fibers (Arends & Voogd, 1989; Winship & Wylie, 2003). Thus, there are two routes by which the LM and nBOR reach the VbC: the direct mossy fiber route and an indirect climbing fiber route via the mcIO (Brecha et al., 1980). The response properties and topography of these olivo-vestibulocerebellar pathways have been studied in great detail (Wylie & Frost, 1991, 1993, 1999*a*, 1999*b*; Wylie et al., 1993, 1998*a*, 1999, 2003*a*, 2003*b*; Lau et al., 1998; Winship & Wylie, 2001, 2003, 2006; Wylie, 2001; Pakan et al., 2005; Winship et al., 2005). Brecha et al. (1980) reported that the projection to IO originated with small fusiform neurons in nBORd and the dorsal parts of nBORp throughout the rostro-caudal extent. Our results corroborate these findings, but with minor variations. We noted that the nBOR neurons labeled from the inferior olive were small, but as likely to be multipolar as fusiform. Second, we noticed a difference in the distribution of cells labeled in the contralateral and ipsilateral nBOR. Those in the contralateral nBOR were relatively localized in the rostral part of the nucleus whereas those in the ipsilateral nBOR were distributed more caudally (Figs. 1A, 1C, 6A, 8). In rats, the homologous projection from the MTN to the IO resembles what we observed in pigeons insofar as the projection to the IO is from cells in the dorsal MTN (Schmidt et al., 1998).

The LM provides an ipsilateral input to IO that is also directed to mcIO (Gamlin & Cohen, 1988; Wylie, 2001). These IO-projecting LM neurons are medium-sized fusiform neurons tightly compacted in circumscribed area on the border of the medial and lateral subnuclei (Pakan et al., 2006). These neurons are larger than their counterparts in nBOR (LM, $223.7 \pm 14.3\ \mu m^2$; nBOR, ipsi, $132.6 \pm 6.4\ \mu m^2$; contra $131.7 \pm 4.6\ \mu m^2$). The IO-projecting LM neurons represented a homogeneous group that was qualitatively and quantitatively distinct from other LM-projection neurons, but the same cannot be said of the IO-projecting nBOR neurons: although significantly smaller than VbC- and OMC-projecting neurons, they were not different from those nBOR neurons projecting to the LM, dorsal thalamus, contralateral nBOR and the midline-mesencephalon.

Projection to the midline-mesencephalon

The nBOR provides input to numerous structures of the AON along the midline of the mesencephalon. It was originally described as a projection to IS (Brecha et al., 1980), the major recipient in the area, but Wylie et al. (1997) showed that several other structures in the region also receive input from axons that branch extensively. It is presumed that this projection is important for visual control of both head and eye movements, given that the AON, (and the IS in particular), project to both OMC (Labandeira-Garcia et al., 1989) and the spinal cord (Webster & Steeves, 1988; Arends et al., 1991). In the present study, we showed that nBOR neurons projecting to this area were small and diffusely distributed in the dorsal regions of the nBOR complex (Figs. 2D, 6C). The LM also projects to midline-mesencephalon structures (Gamlin & Cohen, 1988) and this originates from small neurons (Pakan et al., 2006) that resemble their nBOR counterparts.

Projection to the contralateral nBOR

The projection to the contralateral nBOR is directed mainly to nBORd (Brecha et al., 1980; Wylie et al., 1997). Brecha et al. (1980) reported that this projection originated with medium to large cells mainly in nBORp, but few were found in nBORd. This is one of the few specifics where our data is at odds with that of Brecha et al. (1980). We found that the retrograde labeled neurons were small in size, and not different from those retrograde labeled from injections into IO, midline-mesencephalon, dorsal thalamus, or LM. The nBOR-projecting neurons were located mainly in nBORd and the dorsal part of nBORp (Figs. 2A, 3D, 7A, 7D) and concentrated in the caudal half (Fig. 8). These discrepancies might have to do with the fact that cell measurement is now easier with sophisticated software tools, or that iontophoreses of CTB used in the present study allows for much smaller, more restrictive injections compared to injection of WGA-HRP with a Hamilton syringe.

Projection to the LM

There is a heavy reciprocal connection between LM and nBOR (Clarke, 1977; Brecha et al., 1980; Gamlin & Cohen, 1988; Wylie et al., 1997). From injections into LM, small cells were labeled throughout nBOR, especially in the dorsal two-thirds of nBORp and nBORd. Considering the homologous projection in rats, after injections in the NOT, retrograde labeled cells are found throughout MTN (Schmidt et al., 1998). Our double-labeling studies showed that, although the distribution of the LM-projecting neurons was ventral to that of the contra-nBOR-, dorsal thalamus-, and IO-projecting neurons, there was considerable overlap in nBORd (Figs. 3B, 3D, 7A–7C). Brecha et al. (1980) reported that large and medium sized cells were labeled in the nBORp and nBORd after injections in LM. Although we noted a similar distribution of retrograde labeled cells, once again our data are at odds with this as we found that small nBOR neurons were labeled after injections in LM (Figs. 2E, 3B, 4, 5).

Projection to the dorsal thalamus

Wylie et al. (1998*b*) described the projection as originating mainly in nBORd, and terminating in several subnuclei in the dorsal thalamus, but mainly the lateral nucleus of the anterior dorslateral thalamus (DLL). DLL is part of the principal optic nucleus of the thalamus and considered to be equivalent to the lateral geniculate nucleus of the mammalian thalamus (e.g., Karten et al., 1973). In the present study, we confirmed that the cells projecting to the dorsal thalamus were located mainly in nBORd, and found that these were small neurons, not significantly different in size from those projecting to IO, LM, contralateral nBOR, and the midline-mesencephalon. In double-labeling studies, pairing injections in the dorsal thalamus with injections in either IO, contralateral nBOR, or LM, no double labeled neurons were observed. In particular, the absence of double-labeling from the case involving the LM was surprising. The axons that travel to the dorsal thalamus course in a large bundle through the LM where the majority terminates. We (Wylie et al., 1997, 1998*b*) had suspected that many of the axons traveling to the dorsal thalamus would give collaterals that terminate in LM.

Proposed functions of the different types of nBOR neurons

The results of the present study, along with previous studies (e.g., Brecha et al., 1980; Zayats et al., 2002), emphasize that the nBOR should not be regarded as a homogeneous structure, but rather consists of morphologically distinct subtypes of neurons with particular projections. The question remains, do different nBOR cell populations have different physiological properties and differential functional correlates? A few studies are beginning to address the various roles of the different cell types in visual information processing. For example, using double-labeling retrograde techniques combined with recordings in vitro, Prochnow et al. (2007) found that neurons in the rat NOT that project to both the contralateral NOT and the ipsilateral superior colliculus have different electrophysiological properties from those that project to IO. They proposed that the former are involved in monitoring visual activity during saccades whereas the latter are involved in the optokinetic response to reduce retinal slip. Below, we offer an assessment of the function of the various cell types in nBOR, much as Pakan et al. (2006) did so for the LM. One of the key observations that we consider is that Zayats et al. (2002) noted that small neurons in the nBOR are GABAergic. Although they considered these to be interneurons, based on functional and comparative considerations, we propose that some of these may give rise to various projections.

Function of nBOR neurons projecting to the inferior olive and vestibulocerebellum

There are two routes from the nBOR to the VbC: large multipolar neurons project directly to the VbC as mossy fibers, and small neurons project to the medial column of the IO, which projects to the VbC as climbing fibers. The olivo-cerebellar pathway projecting to the VbC and originating in the pretectum and accessory optic systems has been studied in detail in numerous species (Simpson, 1984; Simpson et al., 1988*a*; Giolli et al., 2005). The small IO-projecting neurons in nBOR are likely not GABAergic. In rats, Schmidt et al. (1998) unequivocally showed that MTN neurons projecting to IO are not GABAergic. It is not known what neurotransmitter is involved with this projection, although it is not catecholaminergic in pigeons (Winship et al., 2006) or rats (Fallon et al., 1984).

For LM, Pakan et al. (2006) proposed a differential role of the large neurons projecting to the VbC as opposed to the medium-sized neurons projecting to the IO. We propose the same argument for their nBOR counterparts. The complex spike activity (CSA) of VbC Purkinje cells (which reflects CF input: Eccles et al., 1966), responds best to particular patterns of optic flow resulting from either self-translation or self-rotation (birds: Wylie & Frost, 1991, 1993, 1999*a*, 1999*b*; Wylie et al., 1993, 1998*a*; Graf et al., 1988), and these neurons are critical for mediating the optokinetic response (e.g., Robinson, 1976; Zee et al., 1981; Ito et al., 1982; Nagao, 1983; Waespe et al., 1983; Lisberger et al., 1984). CSA of VbC Purkinje cells responds to slow speed of stimulus motion, whereas visually driven mossy fiber activity in the VbC responds to either slow or fast speeds (Winship et al., 2005). Crowder and Wylie (2001) recorded from nBOR neurons and noted that most responded to slowly moving stimuli, but some responded to fast speeds. It follows that the small nBOR neurons projecting to the IO are responsive to slow speed, whereas the large multipolar neurons are responsive to slow or fast stimuli. Following the arguments of Ibbotson et al. (1994) with respect to the role of fast versus slow pretectal neurons, both the small nBOR neurons projecting to IO and the large multipolar VbC-projecting nBOR neurons are involved in processing slow speeds for charging the velocity storage mechanism when retinal slip velocities are low. The large multipolar neurons responding to fast stimuli would be involved when retinal slip velocities are high, such as the latent period at the onset of optokinetic stimulation (see also Wylie & Crowder, 2000).

Functions of the small nBOR neurons

In the present study, we found that small nBOR neurons project to the contralateral nBOR, the midline-mesencephalon, LM and the dorsal thalamus. Zayats et al. (2002) found that small neurons are GABAergic. It follows then that the projections to the above mentioned structures might be, at least in part, GABAergic. Based on comparative and experimental studies, there is support that the projections to the dorsal thalamus and LM are GABAergic. With respect to the nBOR-LM projection, in pigeons Baldo and Britto (1990) found that the nBOR-LM projection is inhibitory, as electrical stimulation of nBOR resulted in a decrease in the activity of LM neurons. By recording from LM after pharmacological inactivation of nBOR, both Gu et al. (2002) and Crowder et al. (2003*b*) concluded that the nBOR-LM projection is largely inhibitory. In

frogs, this projection is, at least in part, GABAergic (Li & Fite, 2001), and several studies in mammals have shown that the MTN to NOT projection is GABAergic (van der Togt et al., 1991; Giolli et al., 1992; van der Togt & Schmidt, 1994). Schmidt et al. (1998) suggest that this projection is almost exclusively GABAergic in rats. Thus, electrophysiological studies show that this projection is inhibitory, and the comparative evidence suggest that it is mediated by GABA. The GABAergic projection from nBOR to LM may represent a critical step in creating fully motion opponent responses. Most LM neurons are fully motion opponent in that they exhibit excitation to motion in one (the preferred) direction and are inhibited by motion in the opposite (anti-preferred) direction. In the basic delay-and-compare motion detector, which has been used to model NOT, LM and nBOR neurons (Ibbotson et al., 1994; Crowder et al., 2003*a*), motion opponency is established by the "subtraction" or "balance" step. The step of the model involves pooling the responses of two half-detectors with opposite direction preferences. If the output of one of the half-detectors is inhibitory the result is a fully motion opponent response (e.g., Ibbotson et al., 1994; Zanker et al., 1999; Ibbotson & Clifford, 2001). Perhaps the small GABAergic nBOR neurons represent the half-detectors with the inhibitory outputs for the fully motion opponent LM neurons. A similar argument has been proposed for the LM to nBOR connection (Pakan et al., 2006).

With respect to the nBOR to dorsal thalamus projection, Cao et al. (2006) have shown that this projection is inhibitory and mediated by GABA. They concluded that these cells modulate the visual information from the retina to the telencephalon during eye movements. Wylie et al. (1998*b*) suggested that this projection may somehow be involved in distinguishing object-motion from self motion. Frost et al. (1990) emphasized that, whereas the nBOR processes optic flow resulting from self-motion, the thalamofugal and tectofugal systems process local motion, which results from objects moving in the environment. Optic flow is generally interpreted as due to self-motion and is not confused with object-motion. Perhaps the nBOR to dorsal thalamus projection is important in this process. A projection from the MTN to the dorsal lateral geniculate nucleus (dLGN) has not been reported in mammals, but there is a substantial projection from NOT to dLGN. This projection is GABAergic (for review see van der Want et al., 1992). Kenigfest et al. (2004) speculated that the equivalent LM-dorsal thalamus projection in pigeons is also likely GABAergic, and Pakan et al. (2006) came to the same conclusion and suggested it might be important for saccadic suppression. However, Cao et al. (2006) found that the LM-dorsal thalamus projection in pigeons was excitatory, whereas the nBOR-dorsal thalamus projection was inhibitory.

As for the projection of the small neurons to the contralateral nBOR and the midline-mesencephalon, there is little data allowing us to elaborate further on their function at this point, save the following. Both nBOR and LM project to the VTA, which in turn projects to the hippocampus (Casini et al., 1986). Wylie et al. (1999) suggested that the VTA-hippocampus projection might be important for conveying optic flow information for "path integration," a form of spatial navigation whereby an animal can determine spatial relationships such as the origin and destination of motion based on ideothetic cues from self-motion. The hippocampus is critical for this behavior (Foster et al., 1989; Wilson & McNaughton, 1993; McNaughton et al., 1995, 1996; Whishaw et al., 1997; Whishaw & Maaswinkel, 1998). Original studies suggested that ideothetic information for self-motion comes from the vestibular system (McNaughton et al., 1995, 1996; Muller et al., 1996) but Wylie et al. (1999) proposed optic flow as an additional ideothetic cue. This assertion is supported by the fact that both vestibular and visual motion cues influence some place cells in the hippocampus and may thus be used for path integration (Sharp et al., 1995).

Acknowledgments

This research was supported by funding from the Canadian Institute for Health Research (CIHR) and the Natural Sciences and Engineering Research Council of Canada (NSERC) to D.R.W.W. J.M.P.P was supported by a graduate fellowship from NSERC and the Alberta Ingenuity fund (AIF). C.A.E. was supported by summer studentships from NSERC and the Alberta Heritage Foundation for Medical Research (AHFMR). D.R.W.W. was supported by funding from the Canada Research Chairs Program.

References

Arends, J. & Voogd, J. (1989). Topographic aspects of the olivocerebellar system in the pigeon. *Experimental Brain Research* **17**, 52–57.

Arends, J.J., Allan, R.W. & Zeigler, H.P. (1991). Organization of the cerebellum in the pigeon (Columba livia): III. Corticovestibular connections with eye and neck premotor areas. *Journal of Comparative Neurology* **306**, 273–289.

Azevedo, T.A., Cukiert, A. & Britto, L.R. (1983). A pretectal projection upon the accessory optic nucleus in the pigeon: An anatomical and electrophysiological study. *Neuroscience Letter* **43**, 13–18.

Baldo, M.V. & Britto, L.R. (1990). Accessory optic-pretectal interactions in the pigeon. *Brazilian Journal of Medical and Biological Research* **23**, 1037–1040.

Brecha, N., Karten, H.J. & Hunt, S.P. (1980). Projections of the nucleus of the basal optic root in the pigeon: An autoradiographic and horseradish peroxidase study. *Journal of Comparative Neurology* **189**, 615–670.

Burns, S. & Wallman, J. (1981). Relation of single unit properties to the oculomotor function of the nucleus of the basal optic root (accessory optic system) in chickens. *Experimental Brain Research* **42**, 171–180.

Cao, P., Yang, Y. & Wang, S.R. (2006). Differential modulation of thalamic neurons by optokinetic nuclei in the pigeon. *Brain Research* **1069**, 159–165.

Casini, G., Bingman, V.P. & Bagnoli, P. (1986). Connections of the pigeon dorsomedial forebrain studied with WGA-HRP and 3H-proline. *Journal of Comparative Neurology* **245**, 454–470.

Clarke, P.G. (1977). Some visual and other connections to the cerebellum of the pigeon. *Journal of Comparative Neurology* **174**, 535–552.

Clarke, R.J., Giolli, R.A., Blanks, R.H., Torigoe, Y. & Fallon, J.H. (1989). Neurons of the medial terminal accessory optic nucleus of the rat are poorly collateralized. *Visual Neuroscience* **2**, 269–273.

Crowder, N.A., Dawson, M.R. & Wylie, D.R. (2003*a*). Temporal frequency and velocity-like tuning in the pigeon accessory optic system. *Journal of Neurophysiology* **90**, 1829–1841.

Crowder, N.A., Lehmann, H., Parent, M.B. & Wylie, D.R. (2003*b*). The accessory optic system contributes to the spatio-temporal tuning of motion-sensitive pretectal neurons. *Journal of Neurophysiology* **90**, 1140–1151.

Eccles, J.C., Llinas, R., Sasaki, K. & Voorhoeve, P.E. (1966). Interaction experiments on the responses evoked in Purkinje cells by climbing fibres. *Journal of Physiology* **182**, 297–315.

Fallon, J.H., Schmued, L.C., Wang, C., Miller, R. & Banales, G. (1984). Neurons in the ventral tegmentum have separate populations projecting to telencephalon and inferior olive, are histochemically different, and may receive direct visual input. *Brain Research* **321**, 332–336.

Finger, T.E. & Karten, H.J. (1978). The accessory optic system in teleosts. *Brain Research* **153**, 144–149.

Fite, K.V. (1985). Pretectal and accessory-optic visual nuclei of fish, amphibia and reptiles: Theme and variations. *Brain, Behavior and Evolution* **26**, 71–90.

Fite, K.V., Brecha, N., Karten, H.J. & Hunt, S.P. (1981). Displaced ganglion cells and the accessory optic system of pigeon. *Journal of Comparative Neurology* **195**, 279–288.

Fite, K.V., Carey, R.G. & Vicario, D. (1977). Visual neurons in frog anterior thalamus. *Brain Research* **127**, 283–290.

Foster, T.C., Castro, C.A. & McNaughton, B.L. (1989). Spatial selectivity of rat hippocampal neurons: Dependence on preparedness for movement. *Science* **244**, 1580–1582.

Frost, B.J., Wylie, D.R. & Wang, Y.C. (1990). The processing of object and self-motion in the tectofugal and accessory optic pathways of birds. *Vision Research* **30**, 1677–1688.

Gamlin, P.D. (2005). The pretectum: connections and oculomotor-related roles. *Progress in Brain Research* **151**, 379–405.

Gamlin, P.D. & Cohen, D H. (1988). Projections of the retinorecipient pretectal nuclei in the pigeon (Columba livia). *Journal of Comparative Neurology* **269**, 18–46.

Gibson, J.J. (1954). The visual perception of objective motion and subjective movement. *Psychological Review* **61**, 304–314.

Gioanni, H., Rey, J., Villalobos, J. & Dalbera, A. (1984). Single unit activity in the nucleus of the basal optic root (nBOR) during optokinetic, vestibular and visuo-vestibular stimulations in the alert pigeon (Columbia livia). *Experimental Brain Research* **57**, 49–60.

Gioanni, H., Rey, J., Villalobos, J., Richard, D. & Dalbera, A. (1983). Optokinetic nystagmus in the pigeon (Columba livia). II. Role of the pretectal nucleus of the accessory optic system (AOS). *Experimental Brain Research* **50**, 237–247.

Giolli, R.A., Blanks, R.H. & Lui, F. (2005). The accessory optic system: Basic organization with an update on connectivity, neurochemistry, and function. *Progress in Brain Research* **151**, 407–440.

Giolli, R.A., Blanks, R.H. & Torigoe, Y. (1984). Pretectal and brain stem projections of the medial terminal nucleus of the accessory optic system of the rabbit and rat as studied by anterograde and retrograde neuronal tracing methods. *Journal of Comparative Neurology* **227**, 228–251.

Giolli, R.A., Blanks, R.H., Torigoe, Y. & Williams, D.D. (1985). Projections of medial terminal accessory optic nucleus, ventral tegmental nuclei, and substantia nigra of rabbit and rat as studied by retrograde axonal transport of horseradish peroxidase. *Journal of Comparative Neurology* **232**, 99–116.

Giolli, R.A., Torigoe, Y. & Blanks, R.H. (1988). Nonretinal projections to the medial terminal accessory optic nucleus in rabbit and rat: A retrograde and anterograde transport study. *Journal of Comparative Neurology* **269**, 73–86.

Giolli, RA., Torigoe, Y., Clarke, R.J., Blanks, R.H. & Fallon, J.H. (1992). GABAergic and non-GABAergic projections of accessory optic nuclei, including the visual tegmental relay zone, to the nucleus of the optic tract and dorsal terminal accessory optic nucleus in rat. *Journal of Comparative Neurology* **319**, 349–358.

Gottlieb, M.D. & McKenna, O.C. (1986). Light and electron microscopic study of an avian pretectal nucleus, the lentiform nucleus of the mesencephalon, magnocellular division. *Journal of Comparative Neurology* **248**, 133–145.

Graf, W., Simpson, J.I. & Leonard, C.S. (1988). Spatial organization of visual messages of the rabbit's cerebellar flocculus. II. Complex and simple spike responses of Purkinje cells. *Journal of Neurophysiology* **60**, 2091–2121.

Grasse, K. & Cynader, M. (1990). The accessory optic system in frontal-eyed animals. In *Vision and Visual Dysfunction, Vol. IV, The Neuronal Basis of Visual Function*. New York: MacMillan.

Gu, Y., Wang, Y. & Wang, S.R. (2002). Visual responses of neurons in the nucleus of the basal optic root to stationary stimuli in pigeons. *Journal of Neuroscience Research* **67**, 698–704.

Haines, D.E. & Sowa, T.E. (1985). Evidence of a direct projection from the medial terminal nucleus of the accessory optic system to lobule IX of the cerebellar cortex in the tree shrew (Tupaia glis). *Neuroscience Letter* **55**, 125–130.

Ibbotson, M.R. & Clifford, C.W. (2001). Interactions between ON and OFF signals in directional motion detectors feeding the not of the wallaby. *Journal of Neurophysiology* **86**, 997–1005.

Ibbotson, M.R., Mark, R.F. & Maddess, T.L. (1994). Spatiotemporal response properties of direction-selective neurons in the nucleus of the optic tract and dorsal terminal nucleus of the wallaby, Macropus eugenii. *Journal of Neurophysiology* **72**, 2927–2943.

Ito, M., Orlov, I. & Yamamoto, M. (1982). Topographical representation of vestibulo-ocular reflexes in rabbit cerebellar flocculus. *Neuroscience* **7**, 1657–1664.

Iwaniuk, A.N. & Wylie, D.R. (2007). Neural specialization for hovering in hummingbirds: Hypertrophy of the pretectal nucleus *Lentiformis mesencephali*. *Journal of Comparative Neurology* **500**, 211–221.

Karten, H. & Hodos, W. (1967). *A stereotaxic Atlas of the Brain of the Pigeon (Columba livia)*. Baltimore: Johns Hopkins Press.

Karten, H.J., Hodos, W., Nauta, W.J. & Revzin, A.M. (1973). Neural connections of the "visual wulst" of the avian telencephalon. Experimental studies in the piegon (Columba livia) and owl (Speotyto cunicularia). *Journal of Comparative Neurology* **150**, 253–278.

Karten, J.H., Fite, K.V. & Brecha, N. (1977). Specific projection of displaced retinal ganglion cells upon the accessory optic system in the pigeon (Columbia livia). *Proceedings of the National Academy of Sciences* **74**, 1753–1756.

Kawasaki, T. & Sato, Y. (1980). Afferent projection from the dorsal nucleus of the raphe to the flocculus in cats. *Brain Research* **197**, 496–502.

Kenigfest, N., Rio, J.P., Belekhova, M., Reperant, J., Vesselkin, N. & Ward, R. (2004). Pretectal and tectal afferents to the dorsal lateral geniculate nucleus of the turtle: An electron microscopic axon tracing and gamma-aminobutyric acid immunocytochemical study. *Journal of Comparative Neurology* **475**, 107–127.

Labandeira-Garcia, J.L., Guerra-Seijas, M.J., Labandeira-Garcia, J.A. & Jorge-Barreiro, F.J. (1989). Afferent connections of the oculomotor nucleus in the chick. *Journal of Comparative Neurology* **282**, 523–534.

Lappe, M. & Rauschecker, J.P. (1994). Heading detection from optic flow. *Nature* **369**, 712–713.

Lau, K.L., Glover, R.G., Linkenhoker, B. & Wylie, D.R. (1998). Topographical organization of inferior olive cells projecting to translation and rotation zones in the vestibulocerebellum of pigeons. *Neuroscience* **85**, 605–614.

Lee, D.N. & Lishman, R. (1977). Visual control of locomotion. *Scandinavian Journal of Psychology* **18**, 224–230.

Li, Z. & Fite, K.V. (2001). GABAergic visual pathways in the frog Rana pipiens. *Visual Neuroscience* **18**, 457–464.

Lisberger, S.G., Miles, F.A. & Zee, D.S. (1984). Signals used to compute errors in monkey vestibuloocular reflex: Possible role of flocculus. *Journal of Neurophysiology* **52**, 1140–1153.

McKenna, O.C. & Wallman, J. (1981). Identification of avian brain regions responsive to retinal slip using 2-deoxyglucose. *Brain Research* **210**, 455–460.

McKenna, O.C. & Wallman, J. (1985). Accessory optic system and pretectum of birds: Comparisons with those of other vertebrates. *Brain Behavior and Evolution* **26**, 91–116.

McNaughton, B.L., Barnes, C.A., Gerrard, J.L., Gothard, K., Jung, M.W., Knierim, J.J., Kudrimoti, H., Qin, Y., Skaggs, W.E., Suster, M. & Weaver, K.L. (1996). Deciphering the hippocampal polyglot: The hippocampus as a path integration system. *Journal of Experimental Biology* **199**, 173–185.

McNaughton, N., Logan, B., Panickar, K.S., Kirk, I.J., Pan, W.X., Brown, N.T. & Heenan, A. (1995). Contribution of synapses in the medial supramammillary nucleus to the frequency of hippocampal theta rhythm in freely moving rats. *Hippocampus* **5**, 534–545.

Montgomery, N., Fite, K.V. & Bengston, L. (1981). The accessory optic system of Rana pipiens: Neuroanatomical connections and intrinsic organization. *Journal of Comparative Neurology* **203**, 595–612.

Morgan, B. & Frost, B.J. (1981). Visual response characteristics of neurons in nucleus of basal optic root of pigeons. *Experimental Brain Research* **42**, 181–188.

Muller, R.U., Ranck, J.B., Jr. & Taube, J.S. (1996). Head direction cells: Properties and functional significance. *Current Opinions in Neurobiology* **6**, 196–206.

Nagao, S. (1983). Effects of vestibulocerebellar lesions upon dynamic characteristics and adaptation of vestibulo-ocular and optokinetic responses in pigmented rabbits. *Experimental Brain Research* **53**, 36–46.

Pakan, J.M., Krueger, K., Kelcher, E., Cooper, S., Todd, K.G. & Wylie, D.R. (2006). Projections of the nucleus lentiformis mesencephali in pigeons (*Columba livia*): A comparison of the morphology and distribution of neurons with different efferent projections. *Journal of Comparative Neurology* **495**, 84–99.

Pakan, J.M., Todd, K.G., Nguyen, A.P., Winship, I.R., Hurd, P.L., Jantzie, L.L. & Wylie, D.R. (2005). Inferior olivary neurons innervate multiple zones of the flocculus in pigeons (*Columba livia*). *Journal of Comparative Neurology* **486**, 159–168.

Pakan, J.M. & Wylie, D.R. (2006). Two optic flow pathways from the pretectal nucleus lentiformis mesencephali to the cerebellum in pigeons (*Columba livia*). *Journal of Comparative Neurology* **499**, 732–744.

Prochnow, N., Lee, P., Hall, W.C. & Schmidt, M. (2007). In vitro properties of neurons in the rat pretectal nucleus of the optic tract. *Journal of Neurophysiology* **97**, 3574–3584.

Reiner, A., Brecha, N. & Karten, H.J. (1979). A specific projection of retinal displaced ganglion cells to the nucleus of the basal optic root in the chicken. *Neuroscience* **4**, 1679–1688.

Reiner, A. & Karten, H.J. (1978). A bisynaptic retinocerebellar pathway in the turtle. *Brain Research* **150**, 163–169.

Robinson, D.A. (1976). Adaptive gain control of vestibuloocular reflex by the cerebellum. *Journal of Neurophysiology* **39**, 954–969.

Schmidt, M., Van Der Togt, C., Wahle, P. & Hoffmann, K.P. (1998). Characterization of a directional selective inhibitory input from the medial terminal nucleus to the pretectal nuclear complex in the rat. *European Journal of Neuroscience* **10**, 1533–1543.

Sharp, P.E., Blair, H.T., Etkin, D. & Tzanetos, D.B. (1995). Influences of vestibular and visual motion information on the spatial firing patterns of hippocampal place cells. *Journal of Neuroscience* **15**, 173–189.

Shimizu, T. & Karten, H. (1991). *Central Visual Pathways in Retiles and Birds: Evolution of the Visual System*, Vol. 2, London: MacMillan.

Simpson, J.I. (1984). The accessory optic system. *Annual Review of Neuroscience* **7**, 13–41.

Simpson, J.I., Giolli, R.A. & Blanks, R.H. (1988*a*). The pretectal nuclear complex and the accessory optic system. *Reviews of Oculomotor Research* **2**, 335–364.

Simpson, J.I., Leonard, C.S. & Soodak, R.E. (1988*b*). The accessory optic system. Analyzer of self-motion. *New York Academy of Sciences* **545**, 170–179.

Tang, Z.X. & Wang, S.R. (2002). Intracellular recording and staining of neurons in the pigeon nucleus lentiformis mesencephali. *Brain, Behavior and Evolution* **60**, 52–58.

Van Der Togt, C., Nunes Cardozo, B. & Van Der Want, J. (1991). Medial terminal nucleus terminals in the nucleus of the optic tract contain GABA: An electron microscopical study with immunocytochemical double labeling of GABA and PHA-L. *Journal of Comparative Neurology* **312**, 231–241.

Van Der Togt, C. & Schmidt, M. (1994). Inhibition of neuronal activity in the nucleus of the optic tract due to electrical stimulation of the medial terminal nucleus in the rat. *European Journal of Neuroscience* **6**, 558–564.

Van Der Want, J.J., Nunes Cardozo, J.J. & Van Der Togt, C. (1992). GABAergic neurons and circuits in the pretectal nuclei and the accessory optic system of mammals. *Progress in Brain Research* **90**, 283–305.

Veenman, C.L., Reiner, A. & Honig, M.G. (1992). Biotinylated dextran amine as an anterograde tracer for single- and double-labeling studies. *Journal of Neuroscience Methods* **41**, 239–254.

Waespe, W., Cohen, B. & Raphan, T. (1983). Role of the flocculus and paraflocculus in optokinetic nystagmus and visual-vestibular interactions: Effects of lesions. *Experimental in Brain Research* **50**, 9–33.

Weber, J.T. (1985). Pretectal complex and accessory optic system of primates. *Brain Behavior and Evolution* **26**, 117–140.

Webster, D.M. & Steeves, J.D. (1988). Origins of brainstem-spinal projections in the duck and goose. *Journal of Comparative Neurology* **273**, 573–583.

Whishaw, I.Q. & Maaswinkel, H. (1998). Rats with fimbria-fornix lesions are impaired in path integration: A role for the hippocampus in "sense of direction." *Journal of Neuroscience* **18**, 3050–3058.

Whishaw, I.Q., McKenna, J.E. & Maaswinkel, H. (1997). Hippocampal lesions and path integration. *Current Opinions in Neurobiology* **7**, 228–234.

Wild, J.M. (1989). Pretectal and tectal projections to the homologue of the dorsal lateral geniculate nucleus in the pigeon: An anterograde and retrograde tracing study with cholera toxin conjugated to horseradish peroxidase. *Brain Research* **479**, 130–137.

Wild, J.M., Karten, H.J. & Frost, B.J. (1993). Connections of the auditory forebrain in the pigeon (Columba livia). *Journal of Comparative Neurology* **337**, 32–62.

Wilson, M.A. & McNaughton, B.L. (1993). Dynamics of the hippocampal ensemble code for space. *Science* **261**, 1055–1058.

Winfield, J.A., Hendrickson, A. & Kimm, J. (1978). Anatomical evidence that the medial terminal nucleus of the accessory optic tract in mammals provides a visual mossy fiber input to the flocculus. *Brain Research* **151**, 175–182.

Winship, I.R., Crowder, N.A. & Wylie, D.R. (2006). Quantitative reassessment of speed tuning in the accessory optic system and pretectum of pigeons. *Journal of Neurophysiology* **95**, 546–551.

Winship, I.R., Hurd, P.L. & Wylie, D.R. (2005). Spatiotemporal tuning of optic flow inputs to the vestibulocerebellum in pigeons: Differences between mossy and climbing fiber pathways. *Journal of Neurophysiology* **93**, 1266–1277.

Winship, I.R. & Wylie, D.R. (2001). Responses of neurons in the medial column of the inferior olive in pigeons to translational and rotational optic flowfields. *Experimental Brain Research* **141**, 63–78.

Winship, I.R. & Wylie, D.R. (2003). Zonal organization of the vestibulocerebellum in pigeons (Columba livia): I. Climbing fiber input to the flocculus. *Journal of Comparative Neurology* **456**, 127–139.

Winship, I.R. & Wylie, D.R. (2006). Receptive-field structure of optic flow responsive Purkinje cells in the vestibulocerebellum of pigeons. *Visual Neuroscience* **23**, 115–126.

Winterson, B.J. & Brauth, S.E. (1985). Direction-selective single units in the nucleus lentiformis mesencephali of the pigeon (Columba livia). *Experimental Brain Research* **60**, 215–226.

Wylie, D.R. (2001). Projections from the nucleus of the basal optic root and nucleus lentiformis mesencephali to the inferior olive in pigeons (Columba livia). *Journal of Comparative Neurology* **429**, 502–513.

Wylie, D.R., Bischof, W.F. & Frost, B.J. (1998*a*). Common reference frame for neural coding of translational and rotational optic flow. *Nature* **392**, 278–282.

Wylie, D.R., Brown, M.R., Barkley, R.R., Winship, I.R., Crowder, N.A. & Todd, K.G. (2003*a*). Zonal organization of the vestibulocerebellum in pigeons (*Columba livia*): II. Projections of the rotation zones of the flocculus. *Journal of Comparative Neurology* **456**, 140–153.

Wylie, D.R., Brown, M.R., Winship, I.R., Crowder, N.A. & Todd, K.G. (2003*b*). Zonal organization of the vestibulocerebellum in pigeons (*Columba livia*): III. Projections of the translation zones of the ventral uvula and nodulus. *Journal of Comparative Neurology* **465**, 179–194.

Wylie, D.R. & Crowder, N.A. (2000). Spatiotemporal properties of fast and slow neurons in the pretectal nucleus lentiformis mesencephali in pigeons. *Journal of Neurophysiology* **84**, 2529–2540.

Wylie, D.R. & Frost, B.J. (1990). The visual response properties of neurons in the nucleus of the basal optic root of the pigeon: a quantitative analysis. *Experimental Brain Research* **82**, 327–336.

Wylie, D.R. & Frost, B.J. (1991). Purkinje cells in the vestibulocerebellum of the pigeon respond best to either translational or rotational wholefield visual motion. *Experimental Brain Research* **86**, 229–232.

Wylie, D.R. & Frost, B.J. (1993). Responses of pigeon vestibulocerebellar neurons to optokinetic stimulation. II. The 3-dimensional reference frame of rotation neurons in the flocculus. *Journal of Neurophysiology* **70**, 2647–2659.

Wylie, D.R. & Frost, B.J. (1996). The pigeon optokinetic system: visual input in extraocular muscle coordinates. *Visual Neuroscience* **13**, 945–953.

Wylie, D.R. & Frost, B.J. (1999*a*). Complex spike activity of Purkinje cells in the ventral uvula and nodulus of pigeons in response to translational optic flow. *Journal of Neurophysiology* **81**, 256–266.

Wylie, D.R. & Frost, B.J. (1999*b*). Responses of neurons in the nucleus of the basal optic root to translational and rotational flowfields. *Journal of Neurophysiology* **81**, 267–276.

Wylie, D.R., Glover, R.G. & Lau, K.L. (1998*b*). Projections from the accessory optic system and pretectum to the dorsolateral thalamus in the pigeon (*Columbia livia*): A study using both anteretrograde and retrograde tracers. *Journal of Comparative Neurology* **391**, 456–469.

Wylie, D.R., Kripalani, T. & Frost, B.J. (1993). Responses of pigeon vestibulocerebellar neurons to optokinetic stimulation. I. Functional organization of neurons discriminating between translational and rotational visual flow. *Journal of Neurophysiology* **70**, 2632–2646.

Wylie, D.R. & Linkenhoker, B. (1996). Mossy fibres from the nucleus of the basal optic root project to the vestibular and cerebellar nuclei in pigeons. *Neuroscience Letter* **219**, 83–86.

Wylie, D.R., Linkenhoker, B. & Lau, K.L. (1997). Projections of the nucleus of the basal optic root in pigeons (Columba livia) revealed with biotinylated dextran amine. *Journal of Comparative Neurology* **384**, 517–536.

Wylie, D.R., Winship, I.R. & Glover, R.G. (1999). Projections from the medial column of the inferior olive to different classes of rotation-sensitive Purkinje cells in the flocculus of pigeons. *Neuroscience Letter* **268**, 97–100.

Zanker, J.M., Srinivasan, M.V. & Egelhaaf, M. (1999). Speed tuning in elementary motion detectors of the correlation type. *Biological Cybernetics* **80**, 109–116.

Zayats, N., Davies, D.C., Nemeth, A. & Tombol, T. (2002). The intrinsic neuronal organisation of the nucleus of the basal optic root in the domestic chicken: A light and electron microscopic study using anterograde tracers and postembedding GABA-immunostaining. *European Journal of Morphology* **40**, 101–113.

Zayats, N., Eyre, M.D., Nemeh, A. & Tombol, T. (2003). The intrinsic organization of the nucleus lentiformis mesencephali magnocellularis: A light- and electron-microscopic examination. *Cells Tissues Organs* **174**, 194–207.

Zee, D.S., Yamazaki, A., Butler, P.H. & Gucer, G. (1981). Effects of ablation of flocculus and paraflocculus of eye movements in primate. *Journal of Neurophysiology* **46**, 878–899.